Computer-aided detection of subtle signs of early breast cancer: Detection of architectural distortion in mammograms

Rangaraj M. Rangayyan

Department of Electrical and Computer Engineering,
University of Calgary, Calgary, Alberta, CANADA

UNIVERSITY OF CALGARY

screentest
ALBERTA PROGRAM FOR THE EARLY DETECTION OF BREAST CANCER

SCHULICH School of Engineering

DEPARTMENT OF ELECTRICAL AND COMPUTER ENGINEERING

Breast cancer statistics

- Canada: lifetime probability of developing breast cancer is one in 8.8
- Canada: lifetime probability of death due to breast cancer is one in 27
- Prevalence: 1% of all women living with the disease
- Screening mammography has been shown to reduce mortality rates by 30% to 70%

Mammography

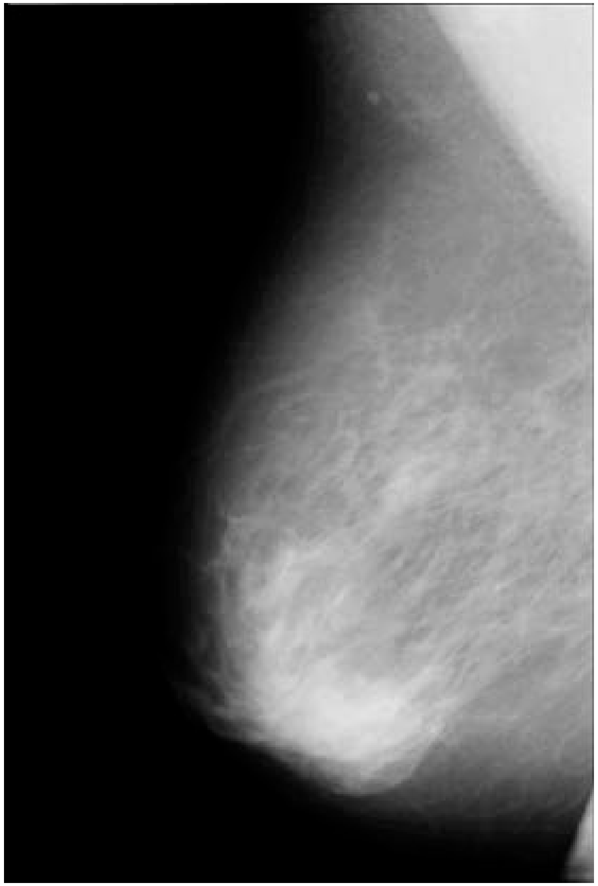

Signs of Breast Cancer:

- Masses
- Calcifications
- Bilateral asymmetry
- Architectural distortion (often missed)

Masses

- Breast cancer causes a desmoplastic reaction in breast tissue
- A mass is observed as a bright, hyper-dense object

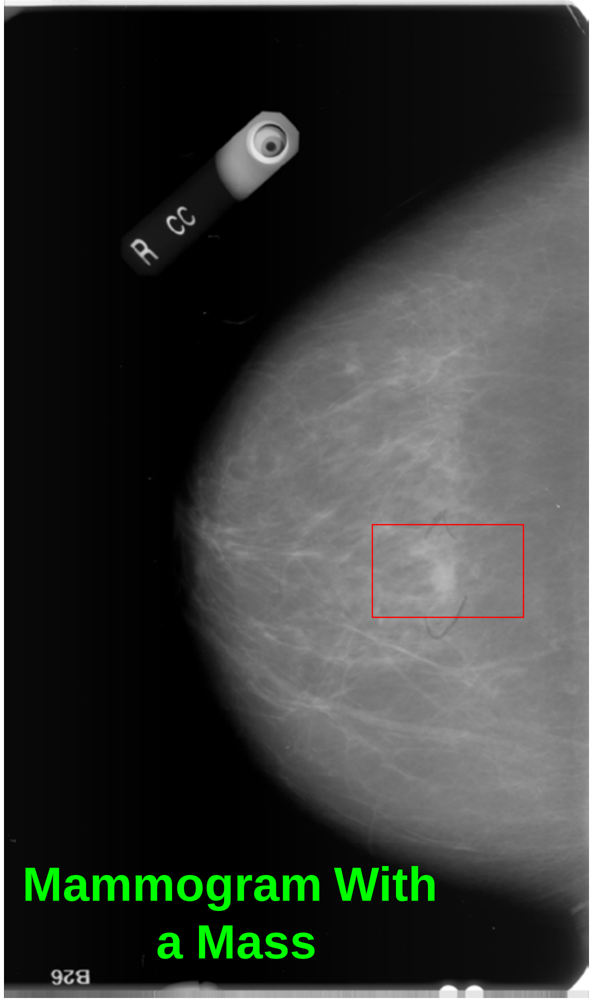

Calcification

Deposits of calcium in breast tissue

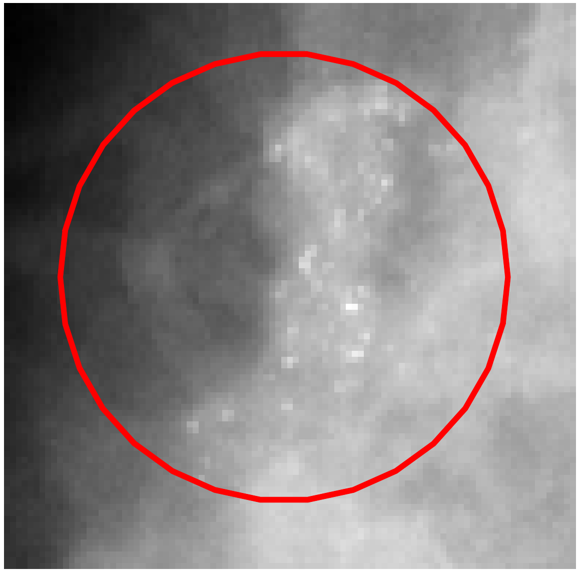

Bilateral asymmetry

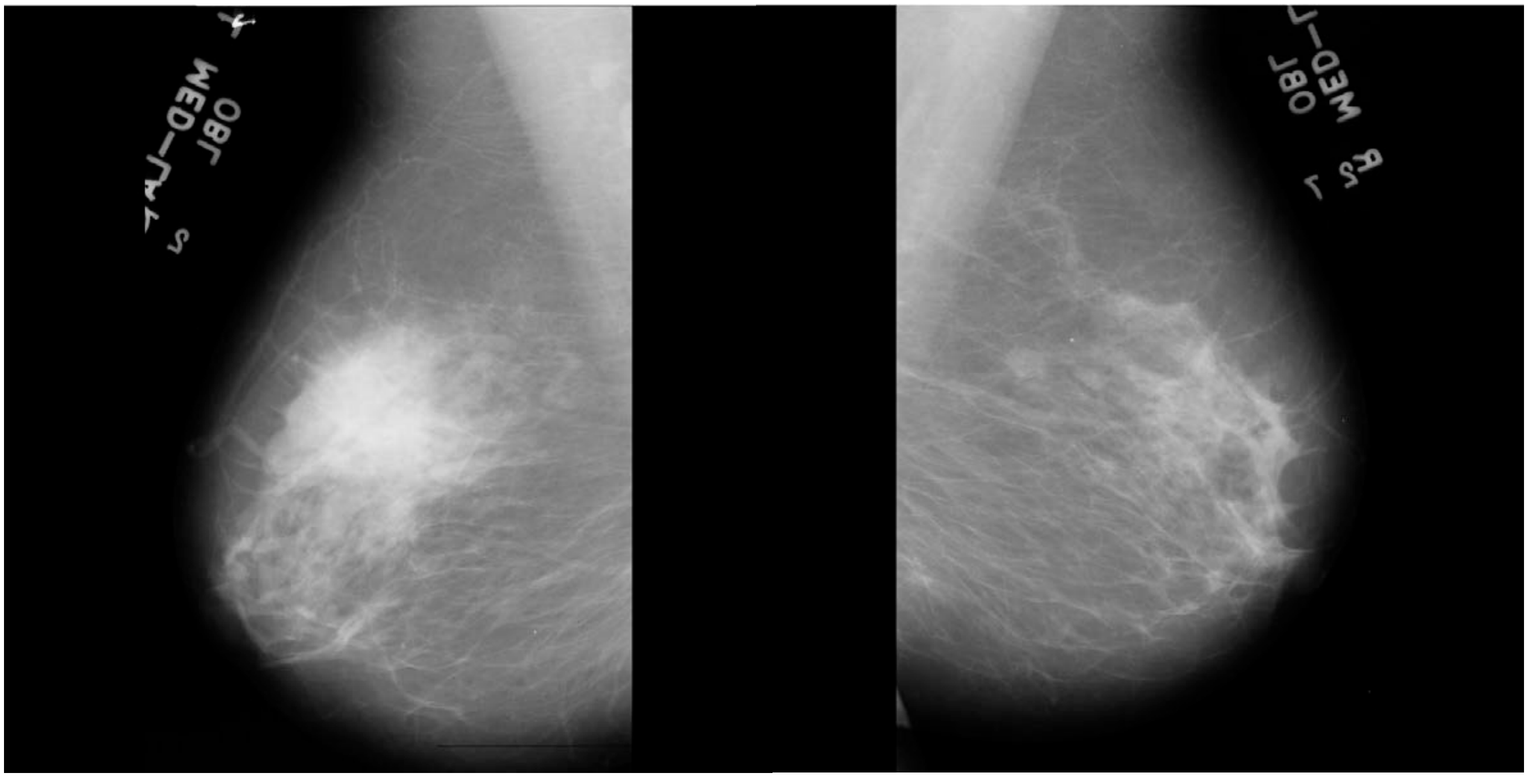

Differences in the overall appearance of one breast with reference to the other

Computer-aided diagnosis

- Increased number of cancers detected[1] by 19.5%
- Increased early-stage malignancies detected[1] from 73% to 78%
- Recall rate increased[1] from 6.5% to 7.7%
- 50% of the cases of architectural distortion missed[2]

[1] *(Freer and Ulissey, 2001)* [2] *(Baker* et al.*, 2003)*

Architectural distortion

- Third most common mammographic sign of nonpalpable breast cancer
- The normal architecture of the breast is distorted
- No definite mass visible
- Spiculations radiating from a point
- Focal retraction or distortion at the edge of the parenchyma

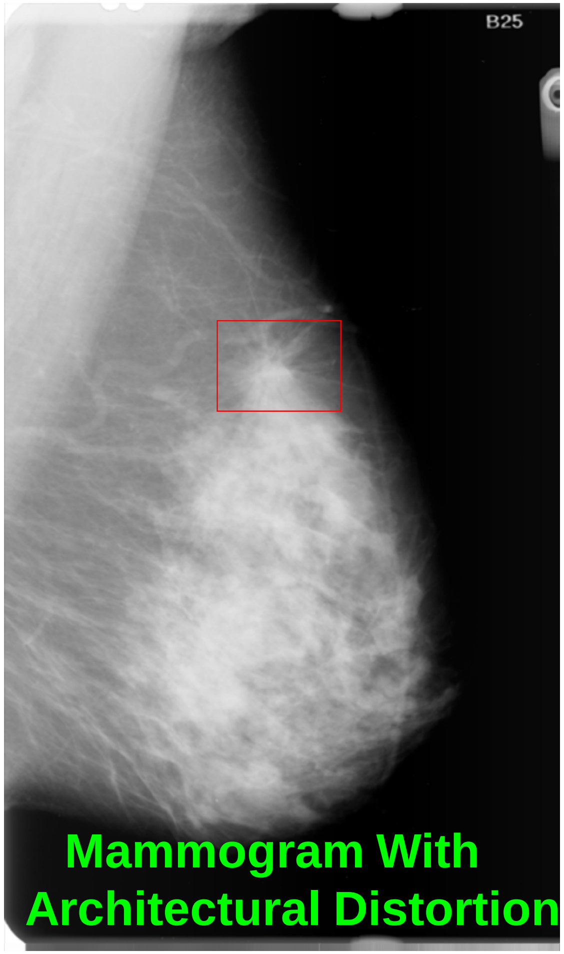

Architectural distortion

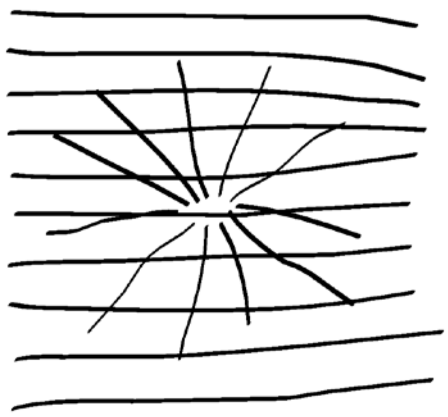

spiculated

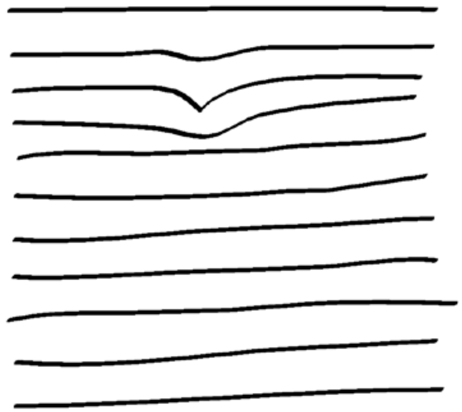

focal retraction

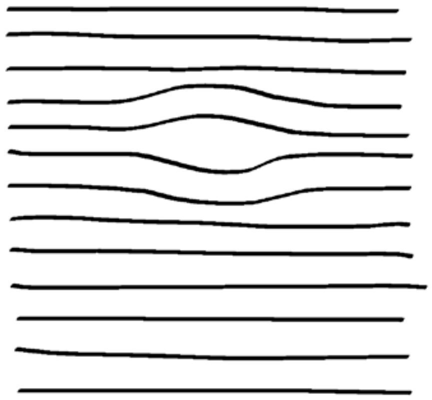

incipient mass

Normal vs. architectural distortion

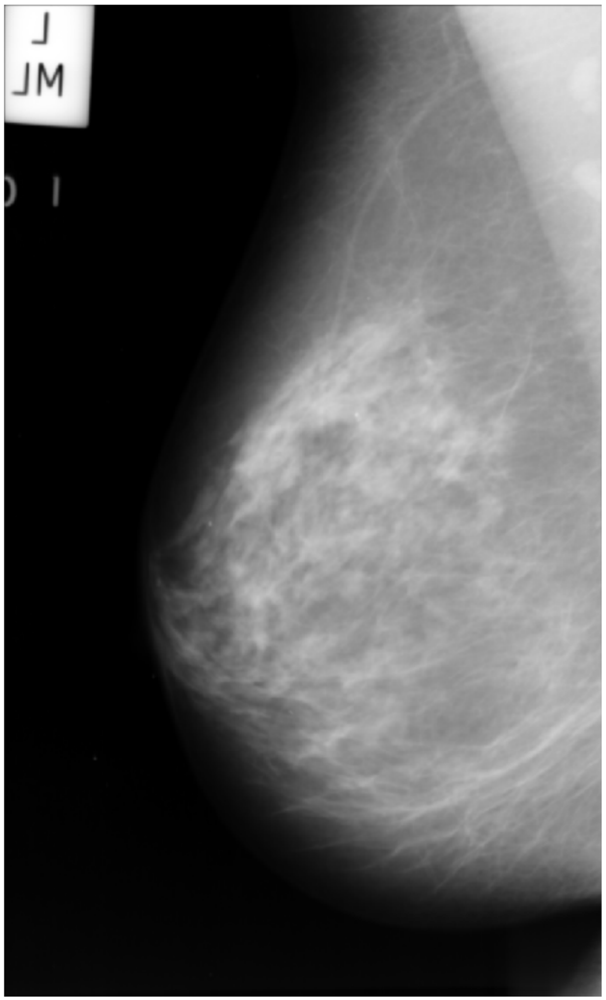

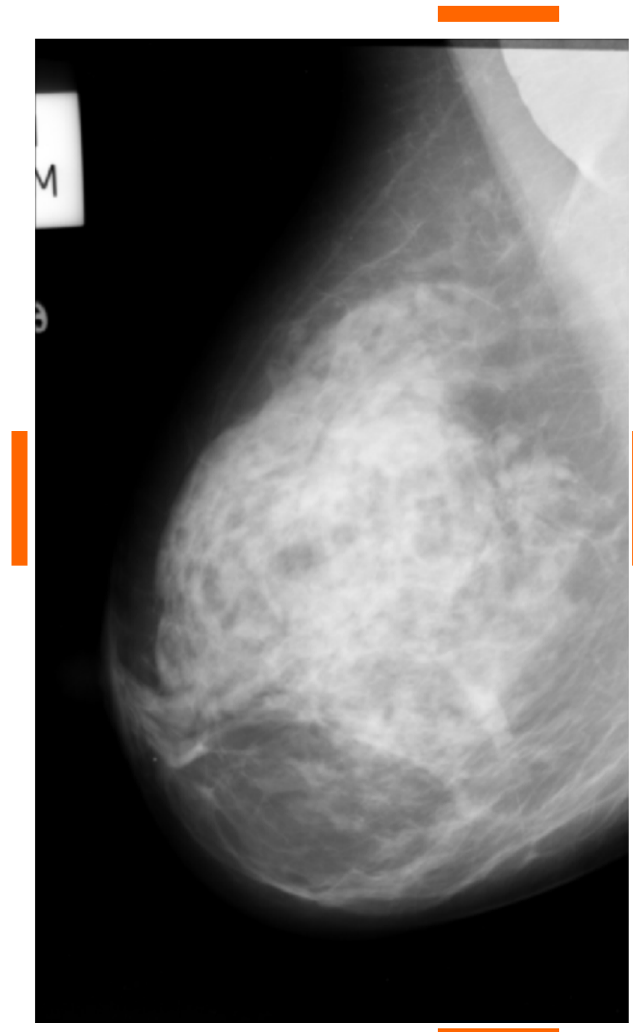

Normal vs. architectural distortion

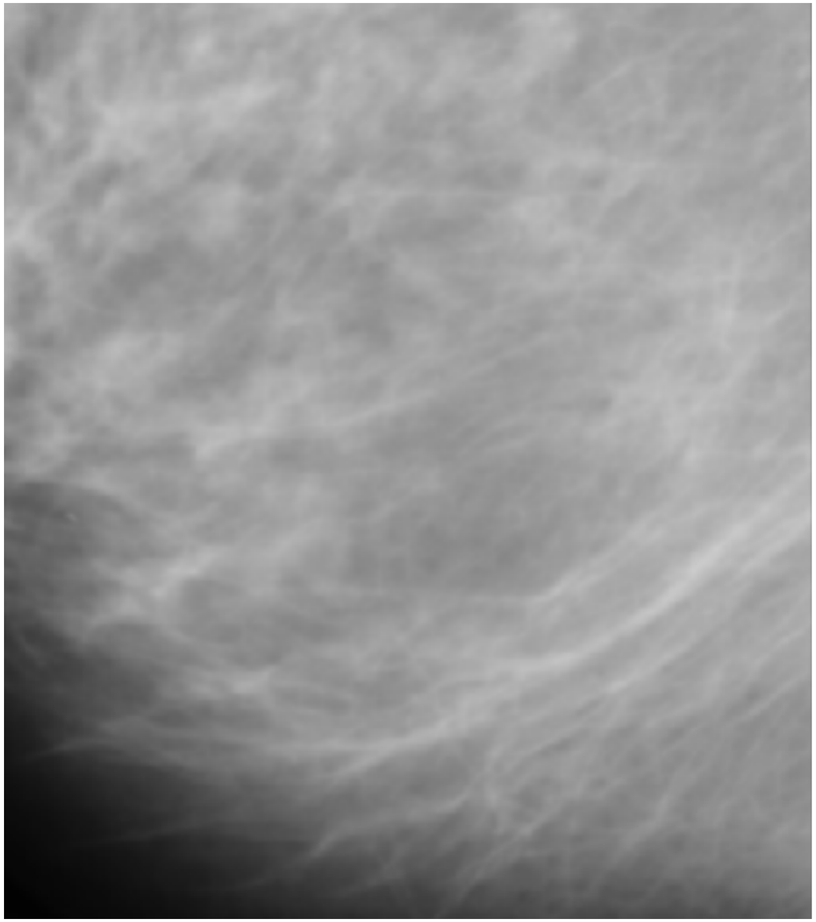

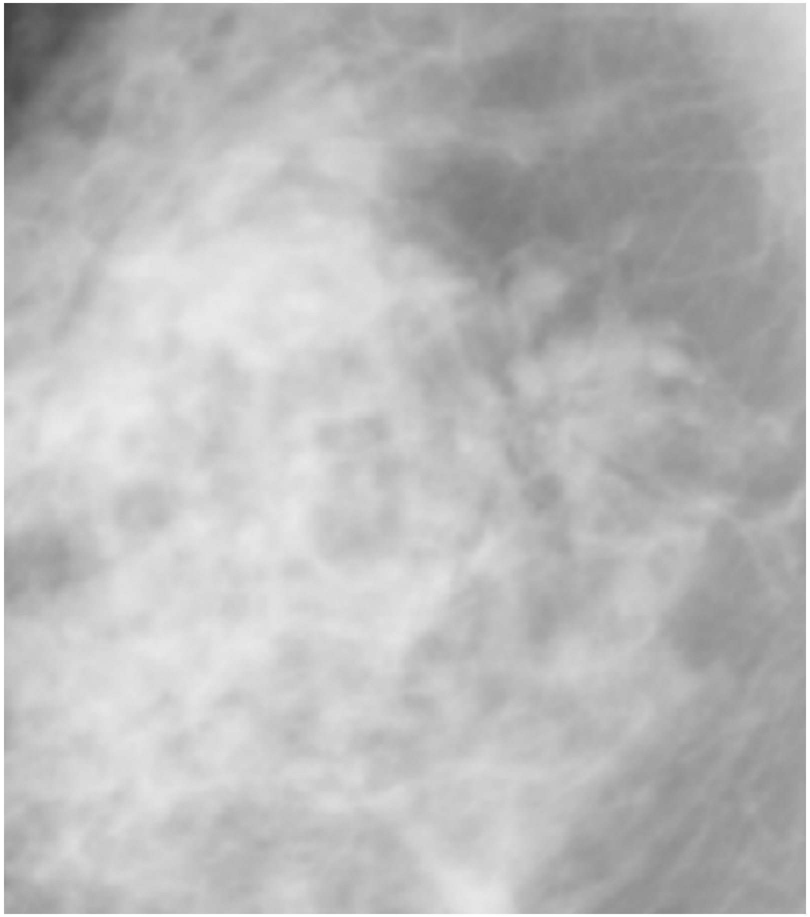

Detection of architectural distortion

1. Extract the orientation field
2. Filter and downsample the orientation field
3. Analyze orientation field using phase portraits
4. Post-process the phase portrait maps
5. Detect sites of architectural distortion

UNIVERSITY OF CALGARY

Gabor filter

$$g(x,y)=\frac{1}{2\pi\sigma_x\sigma_y}\exp\left[-\frac{1}{2}\left(\frac{x^2}{\sigma_x^2}+\frac{y^2}{\sigma_y^2}\right)\right]\cos(2\pi f x)$$

<u>Design parameters</u>

- line thickness τ
- elongation l
- orientation θ

<u>Gabor parameters</u>

$$f=\frac{1}{\tau}; \qquad \sigma_x=\frac{\tau}{2\sqrt{2\ln 2}}$$

$$\sigma_y=l\sigma_x; \quad \begin{bmatrix} x \\ y \end{bmatrix}=\begin{bmatrix} \cos\theta & -\sin\theta \\ \sin\theta & \cos\theta \end{bmatrix}\begin{bmatrix} x' \\ y' \end{bmatrix}$$

Design of Gabor filters

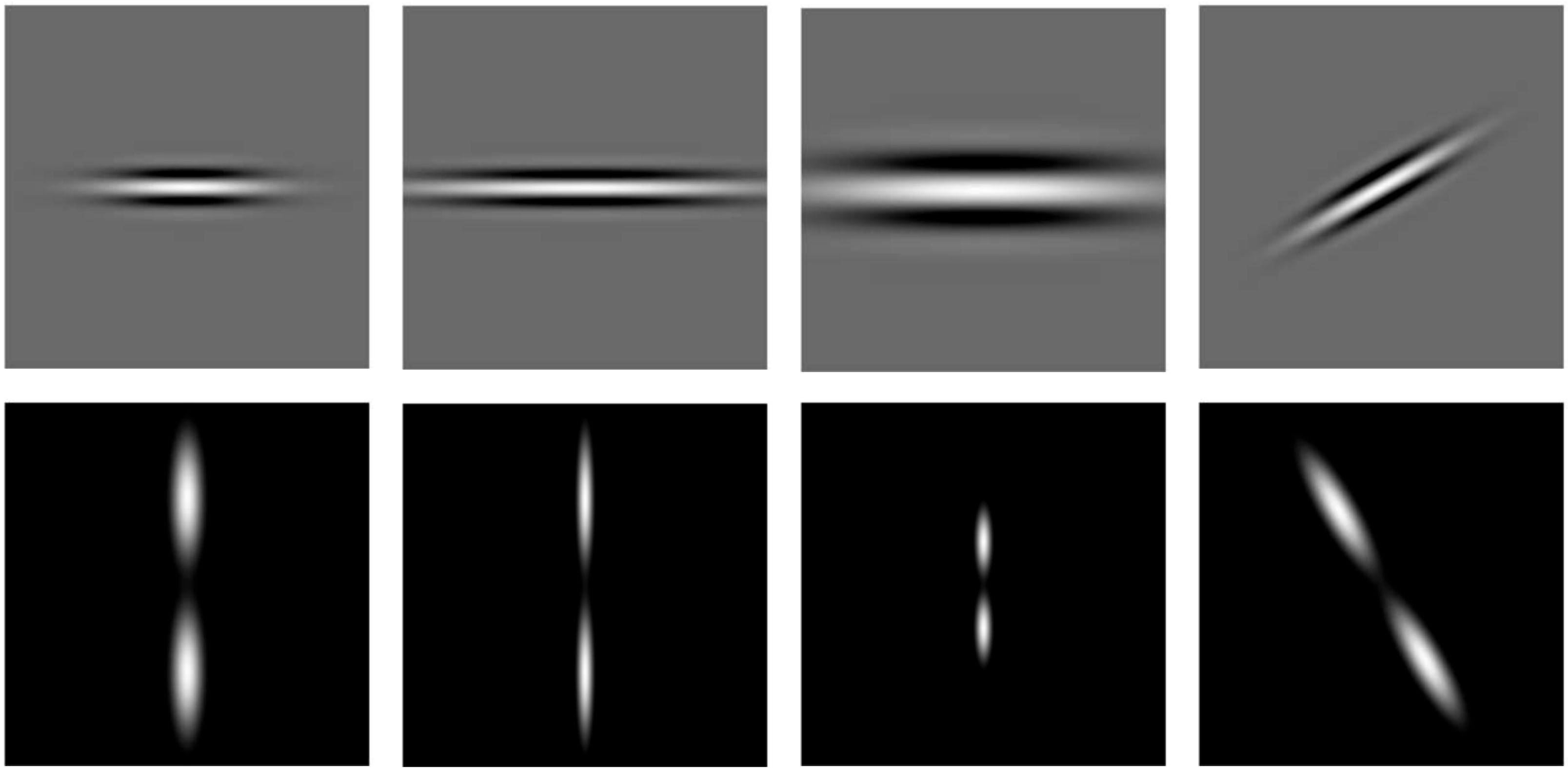

$l = l_0$
$\tau = \tau_0$
$\theta = \theta_0$

$l > l_0$
$\tau = \tau_0$
$\theta = \theta_0$

$l = l_0$
$\tau > \tau_0$
$\theta = \theta_0$

$l = l_0$
$\tau = \tau_0$
$\theta > \theta_0$

Extracting the orientation field

Compute the texture orientation (angle) for each pixel

Gabor filtering
(line detection)

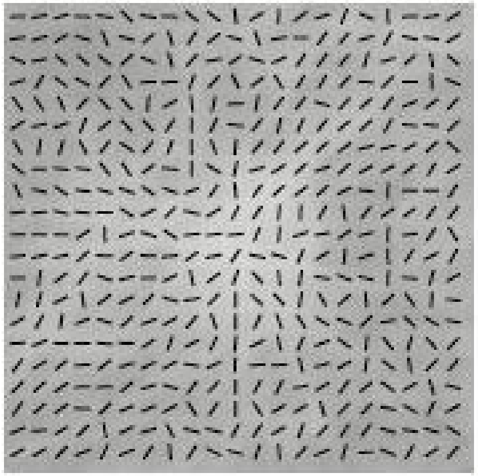

Phase portraits

$$\vec{\boldsymbol{v}}(x,y) = \begin{pmatrix} v_x \\ v_y \end{pmatrix} = \mathbf{A}\begin{pmatrix} x \\ y \end{pmatrix} + \mathbf{b}$$

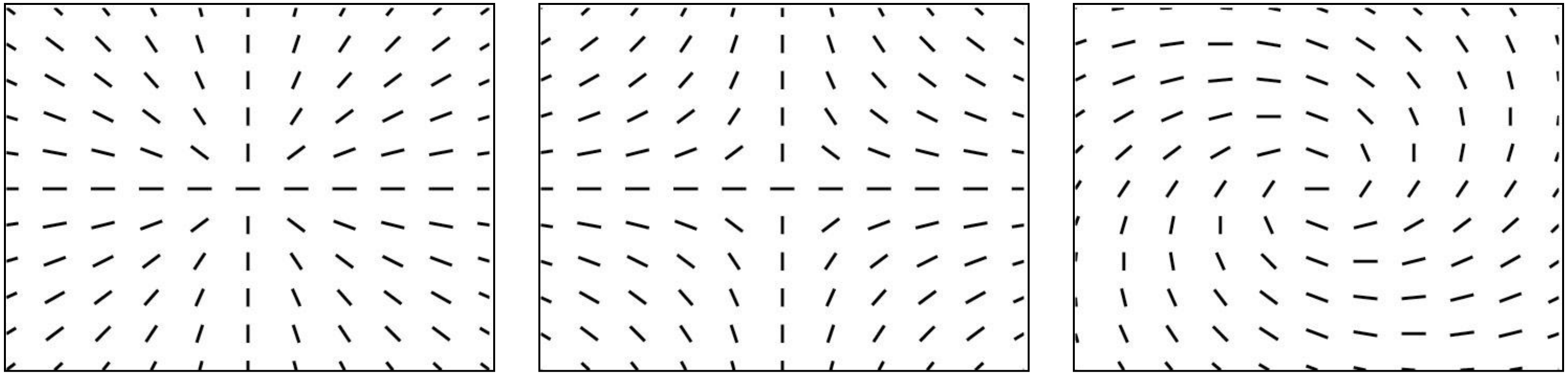

node saddle spiral

Texture analysis using phase portraits

Fit phase portrait model to the analysis window

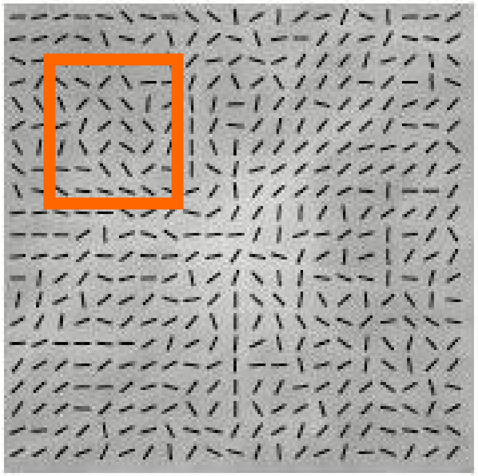

$$\mathbf{A} = \begin{bmatrix} 1.1 & 0.3 \\ -0.2 & 1.7 \end{bmatrix}$$

$$\mathbf{b} = \begin{bmatrix} -4.8 \\ -7.9 \end{bmatrix}$$

Texture analysis using phase portraits

Cast a vote at the fixed point in the corresponding phase portrait map

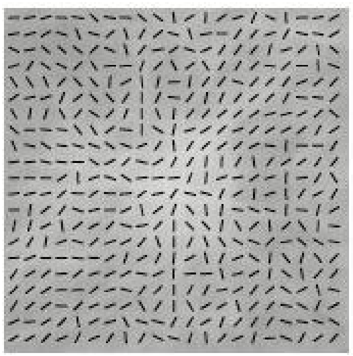

Orientation field

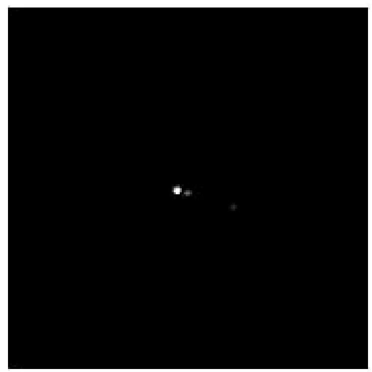

Node

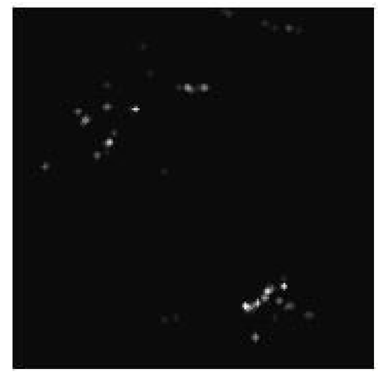

Saddle

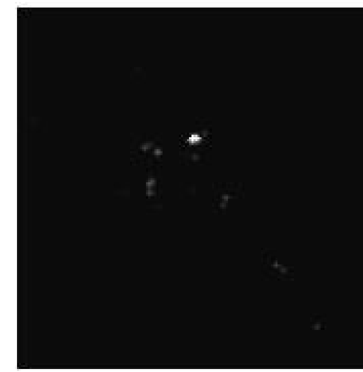

Spiral

Detection of architectural distortion

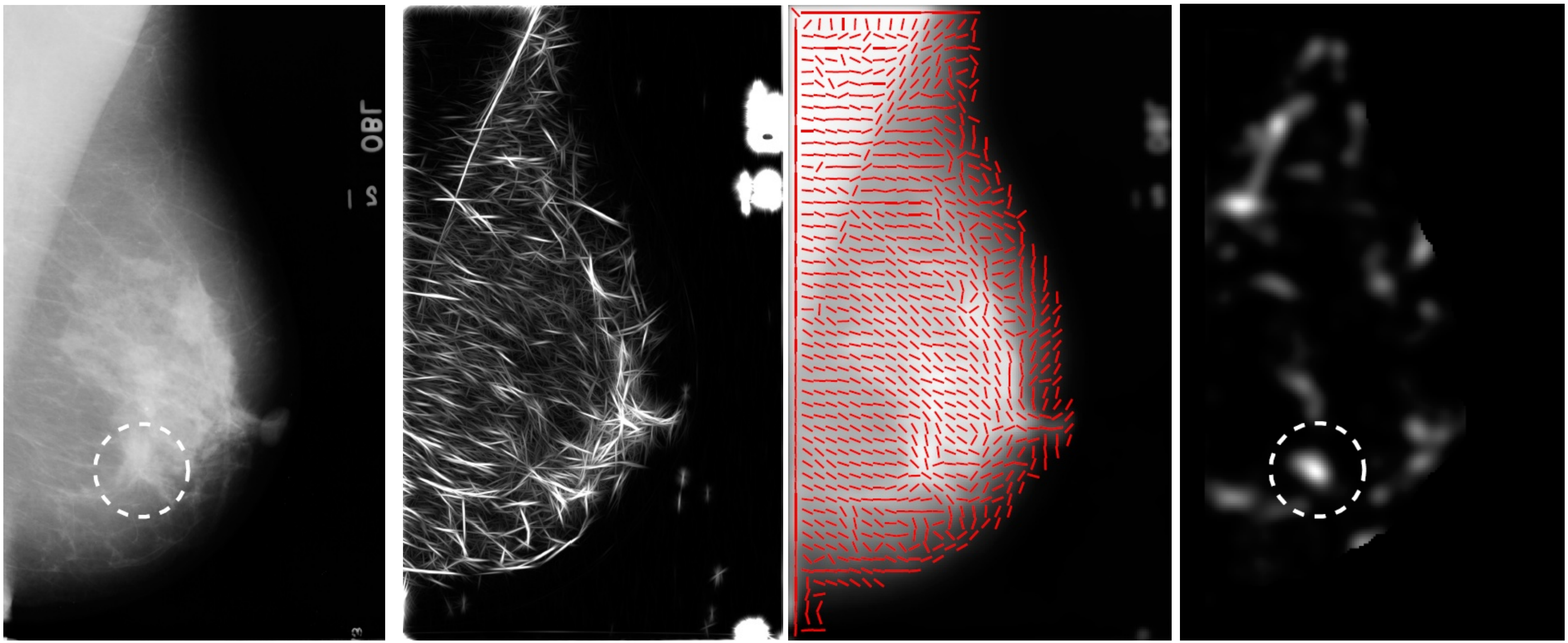

Initial results of detection (2004)

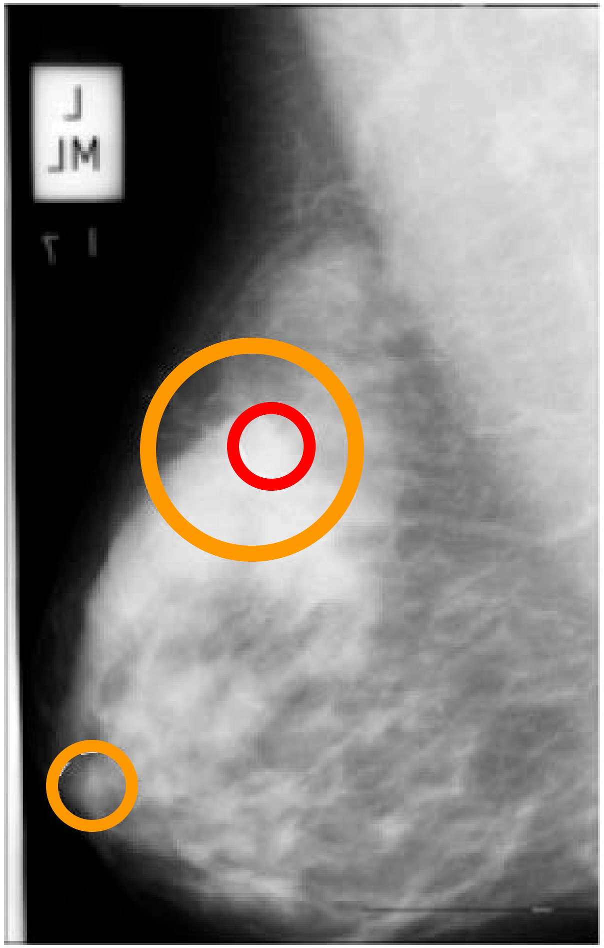

- Test dataset: 19 mammograms with architectural distortion (MIAS database)
- Sensitivity: 84%
- 18 false positives per image

UNIVERSITY OF CALGARY

Reduction of false positives

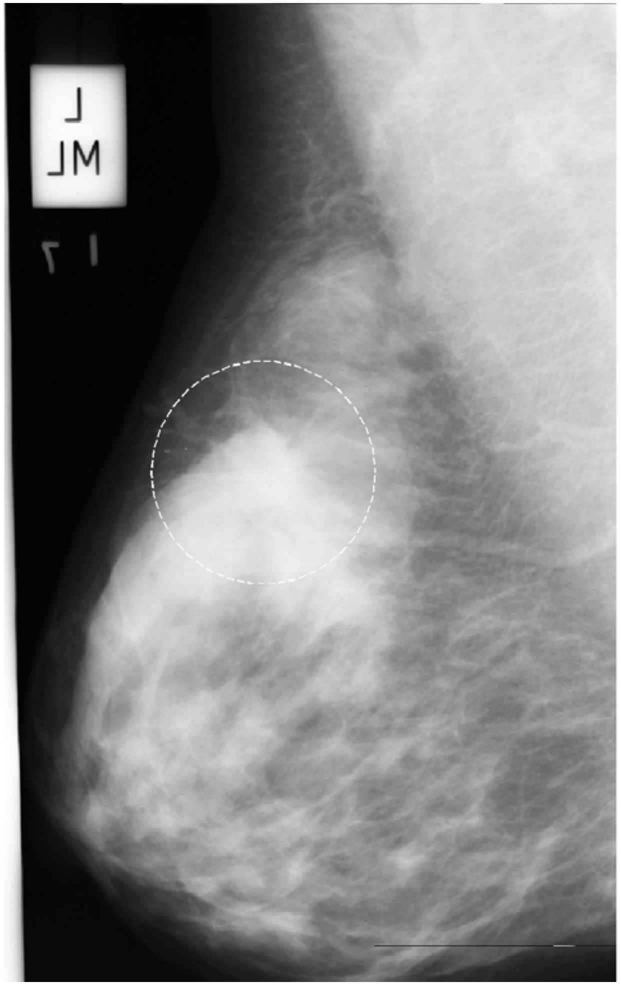

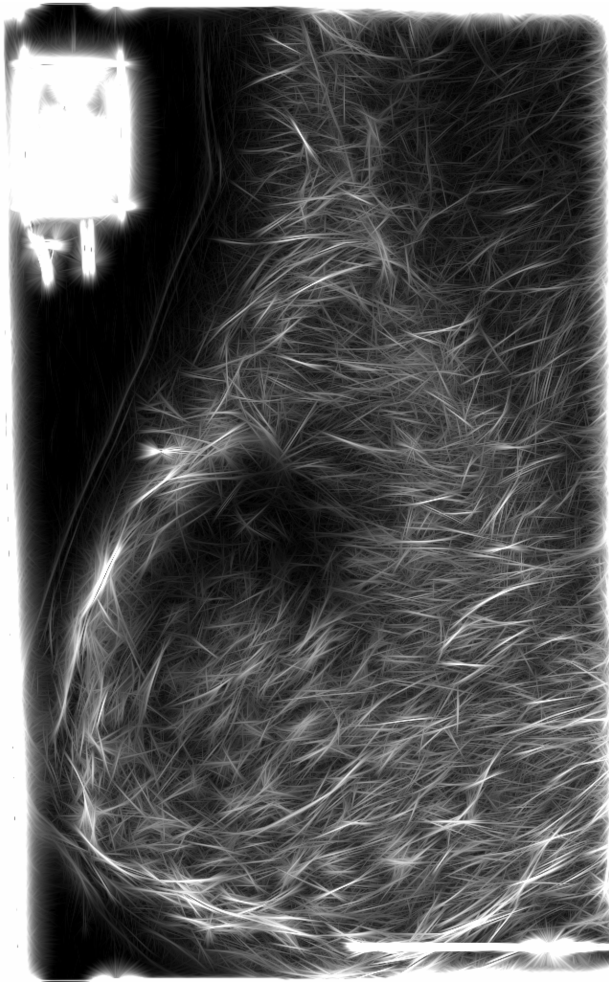

Rejection of confounding structures

- Confounding structures include
  - Edges of vessels
  - Intersections of vessels
  - Edge of the pectoral muscle
  - Edge of the fibro-glandular disk

“Curvilinear Structures”

Nonmaximal suppression

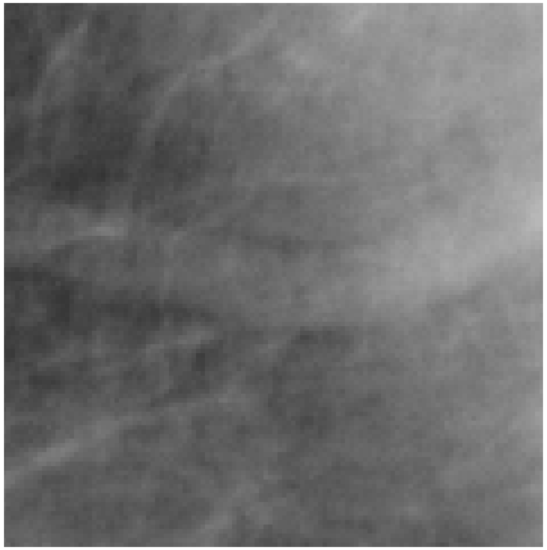

ROI with a vessel

Gabor magnitude output

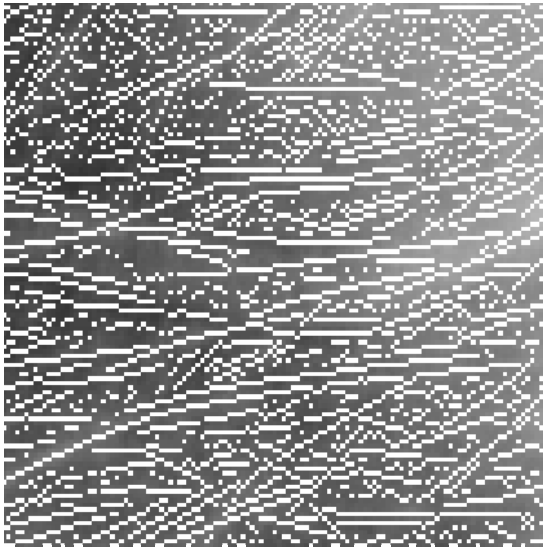

Output of nonmaximal suppression (NMS)

Rejection of confounding CLS

Output of NMS

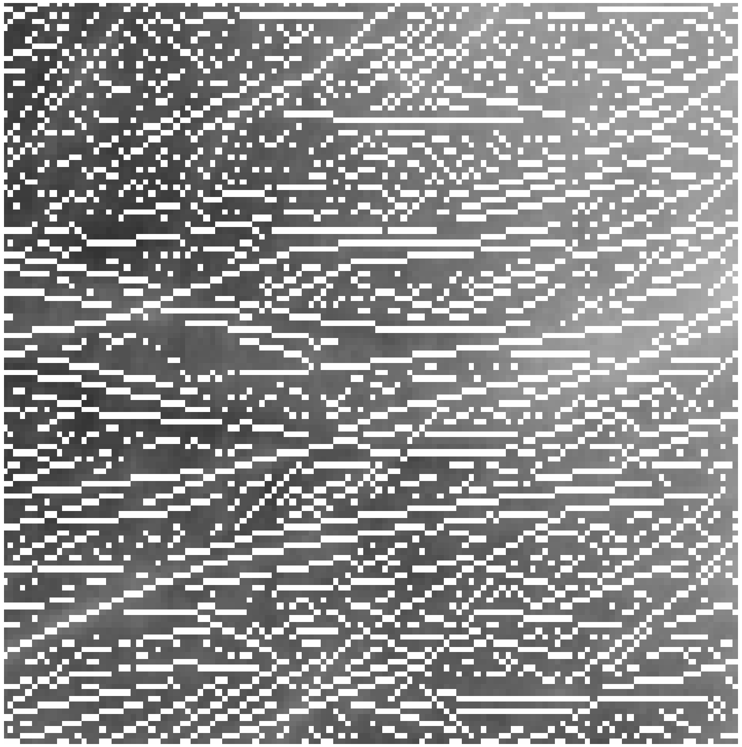

CLS Retained

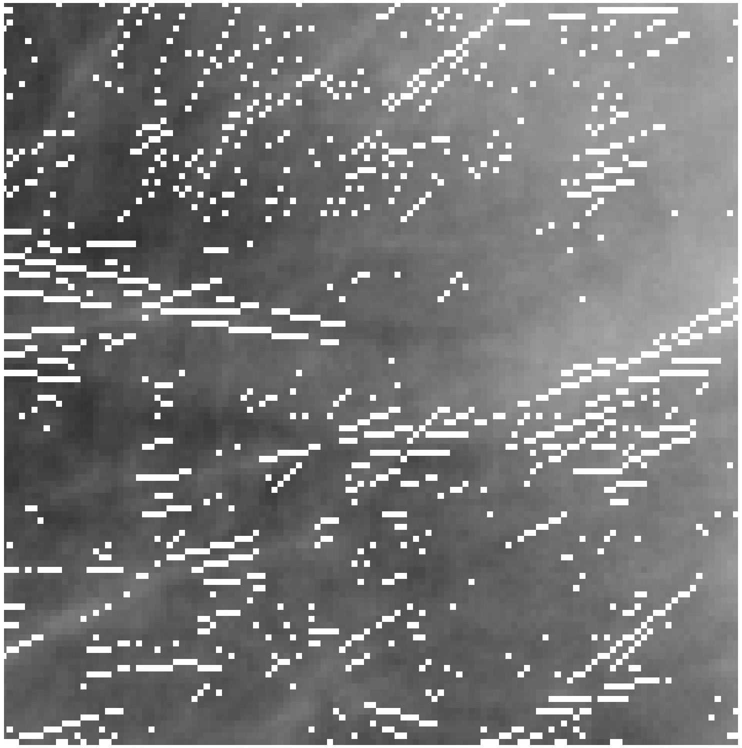

Angle from the orientation field and direction perpendicular to the gradient vector differ by < 30º

Improved detection of sites of architectural distortion

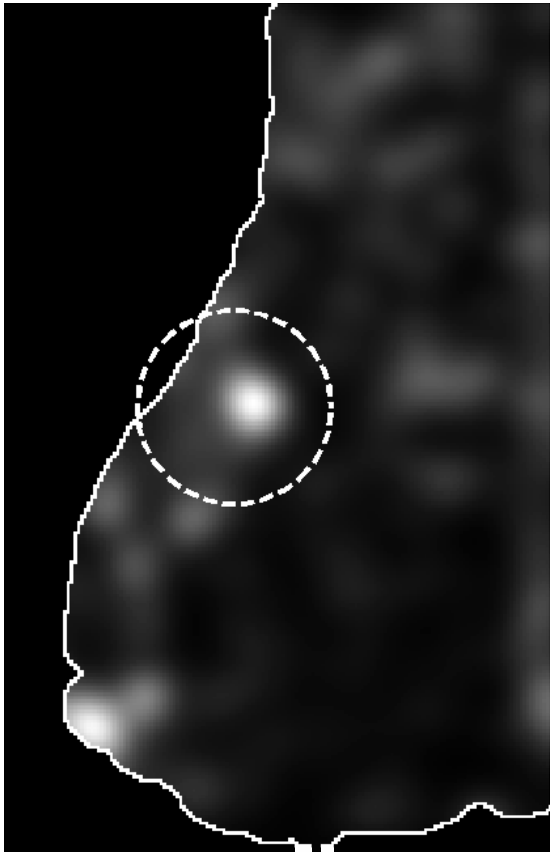

Node map (without CLS analysis)

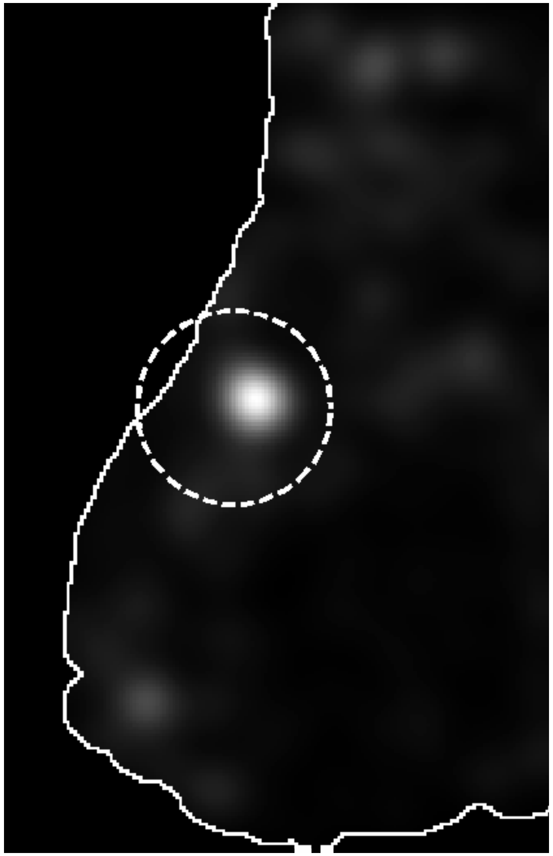

Node map (with CLS analysis)

FROC analysis (2005)

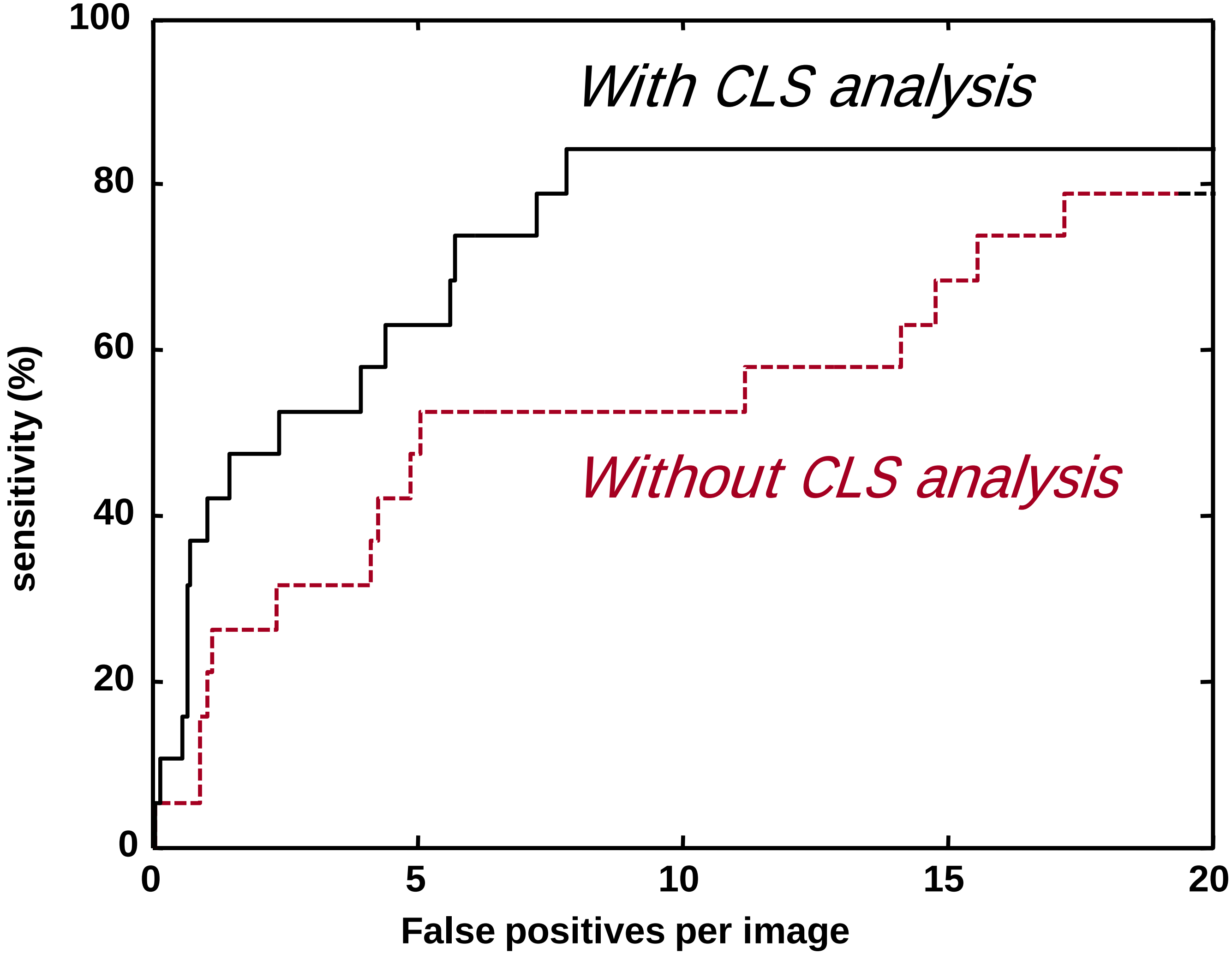

Effect of conditioning number of matrix *A* on the orientation field

Example	Matrix **A**	Eigenvalues	Angle between principal axes	Conditioning number	Orientation field
A	$\begin{bmatrix} 1 & 0 \\ 0 & 3 \end{bmatrix}$	$\lambda_1 = 1$ $\lambda_2 = 3$	90°	3	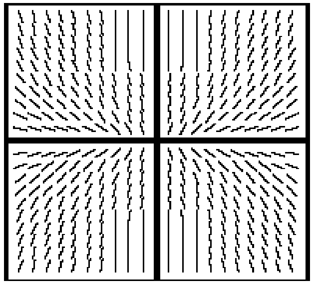
B	$\begin{bmatrix} 1 & 7.46 \\ 0 & 3 \end{bmatrix}$	$\lambda_1 = 1$ $\lambda_2 = 3$	15°	21.85	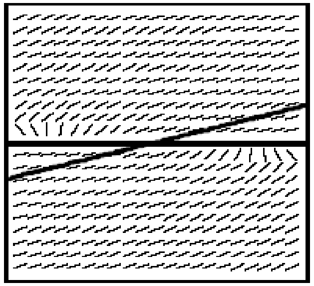
C	$\begin{bmatrix} 1 & 0 \\ 0 & 20 \end{bmatrix}$	$\lambda_1 = 1$ $\lambda_2 = 20$	90°	20	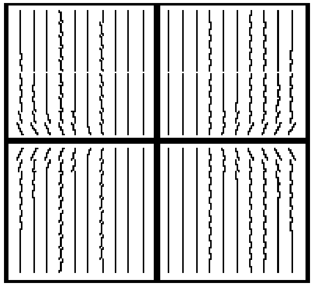

Results (2006)

- 19 cases of architectural distortion
- 41 normal control mammograms (MIAS)

- Symmetric matrix A: node and saddle only
- Conditioning number of $A > 3$: reject result

- *Sensitivity: 84% at 4.5 false positives/image*

- *Sensitivity: 95% at 9.9 false positives/image*

Prior mammograms

Detection mammogram 1997

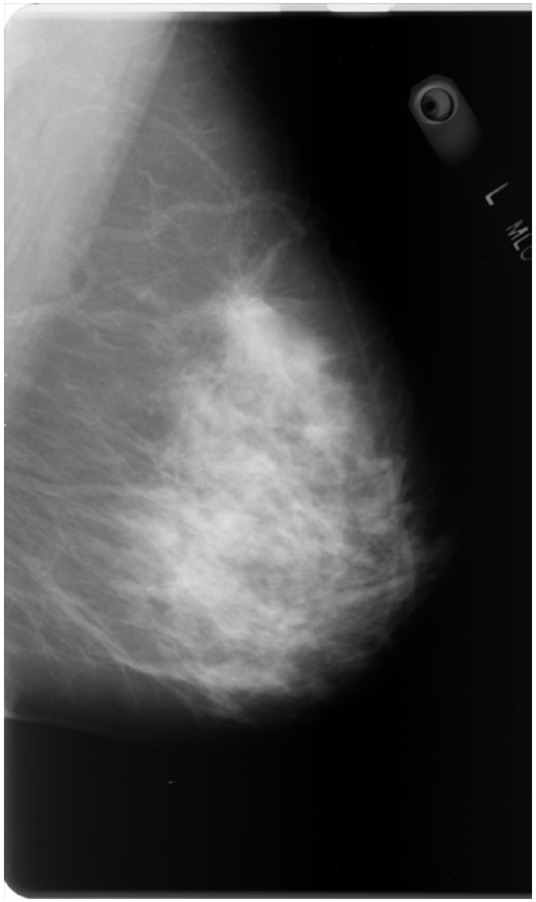

Prior mammogram 1996

Prior mammograms

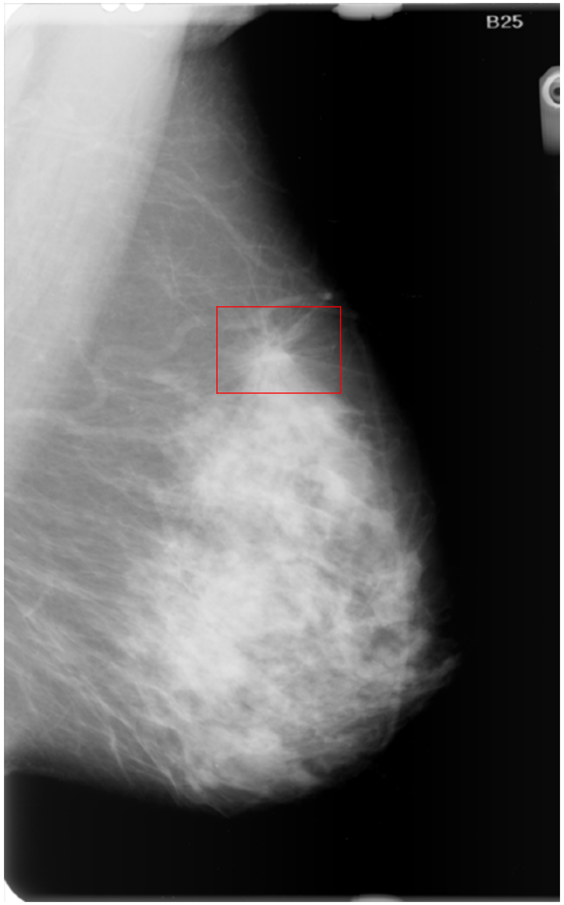

Detection mammogram 1997

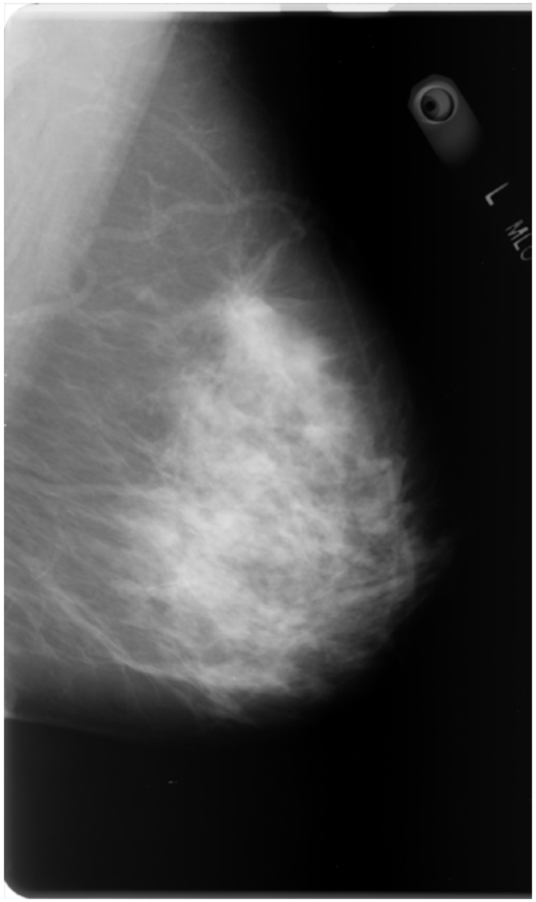

Prior mammogram 1996

UNIVERSITY OF CALGARY

Prior mammograms

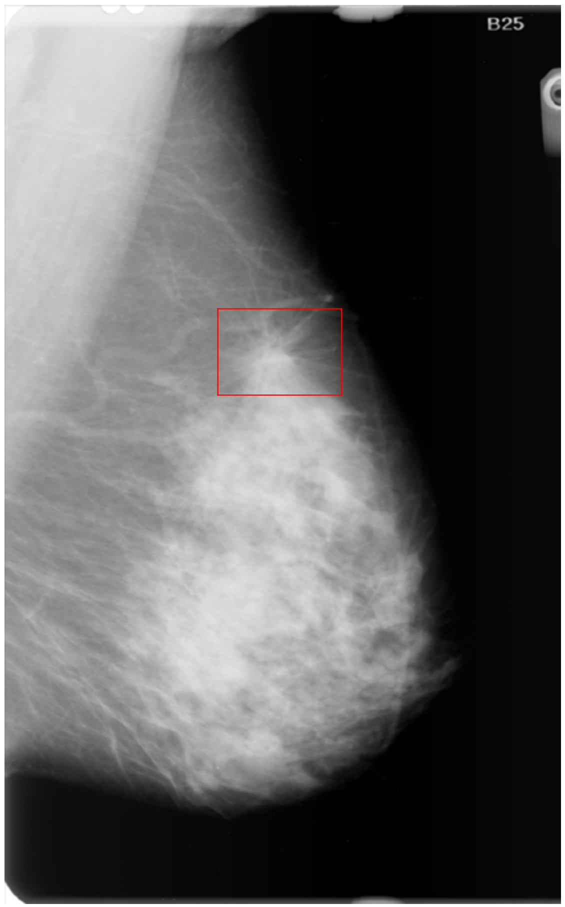

Detection mammogram 1997

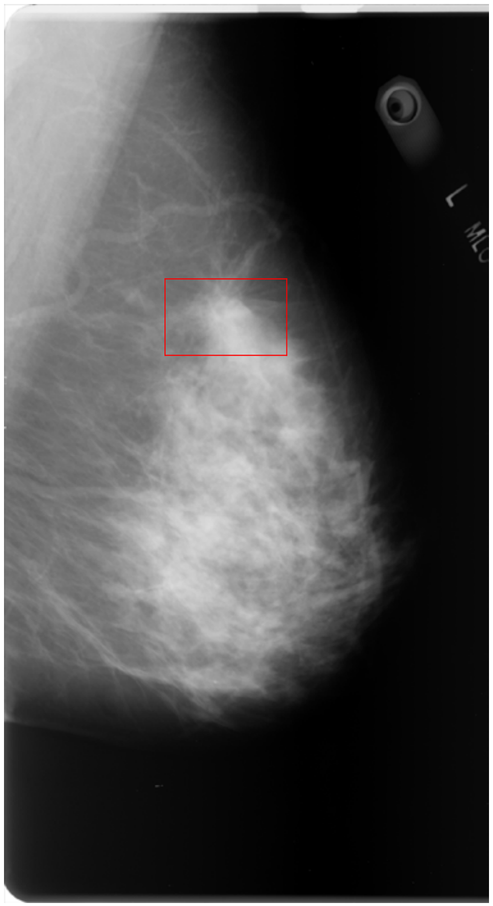

Prior mammogram 1996

Interval cancer

- Indicates a case where breast cancer was detected outside the screening program in the interval between scheduled screening sessions.
- “Detection Mammograms” were not available.

Dataset

- 106 prior mammographic images of 56 individuals diagnosed with breast cancer (interval-cancer cases).
- Time interval between prior and detection (33 cases)- average: 15 months, standard deviation: 7 months, minimum: 1 month, maximum: 24 months.
- 52 prior mammographic images of 13 normal individuals.
- Normal control cases selected represent the penultimate screening visits at the time of preparation of the database.

Interval cancer: site of architectural distortion

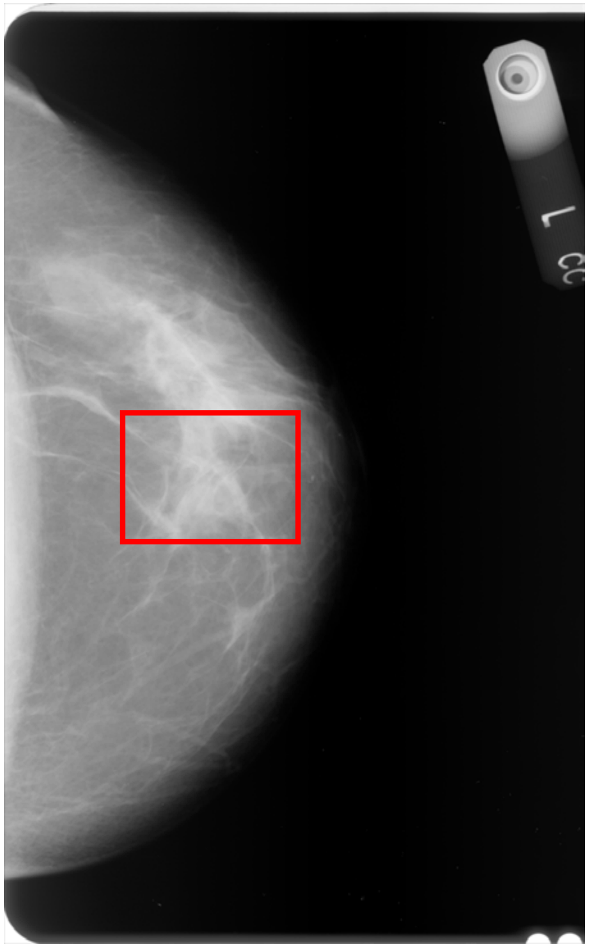

Mammogram

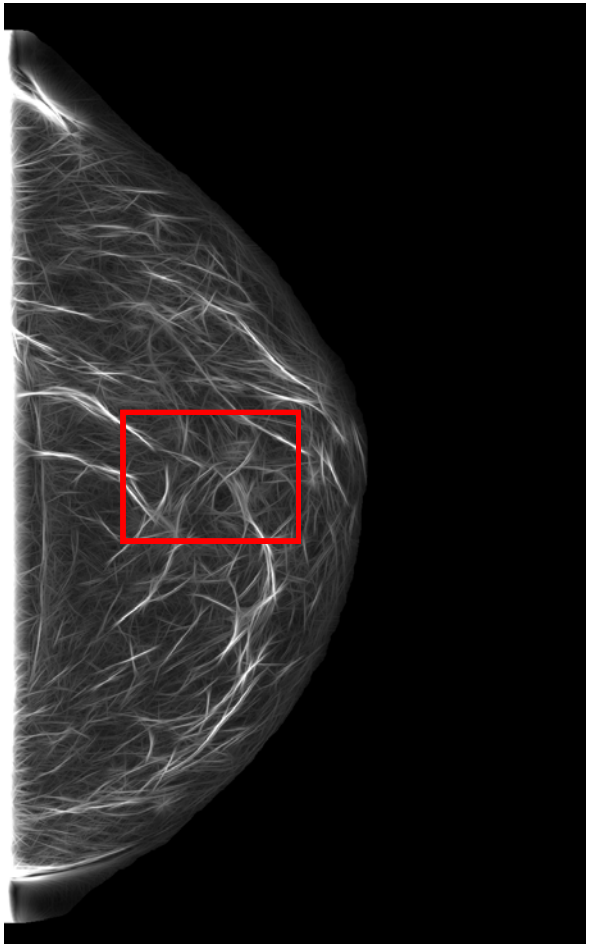

Gabor Magnitude

Interval cancer: site of architectural distortion

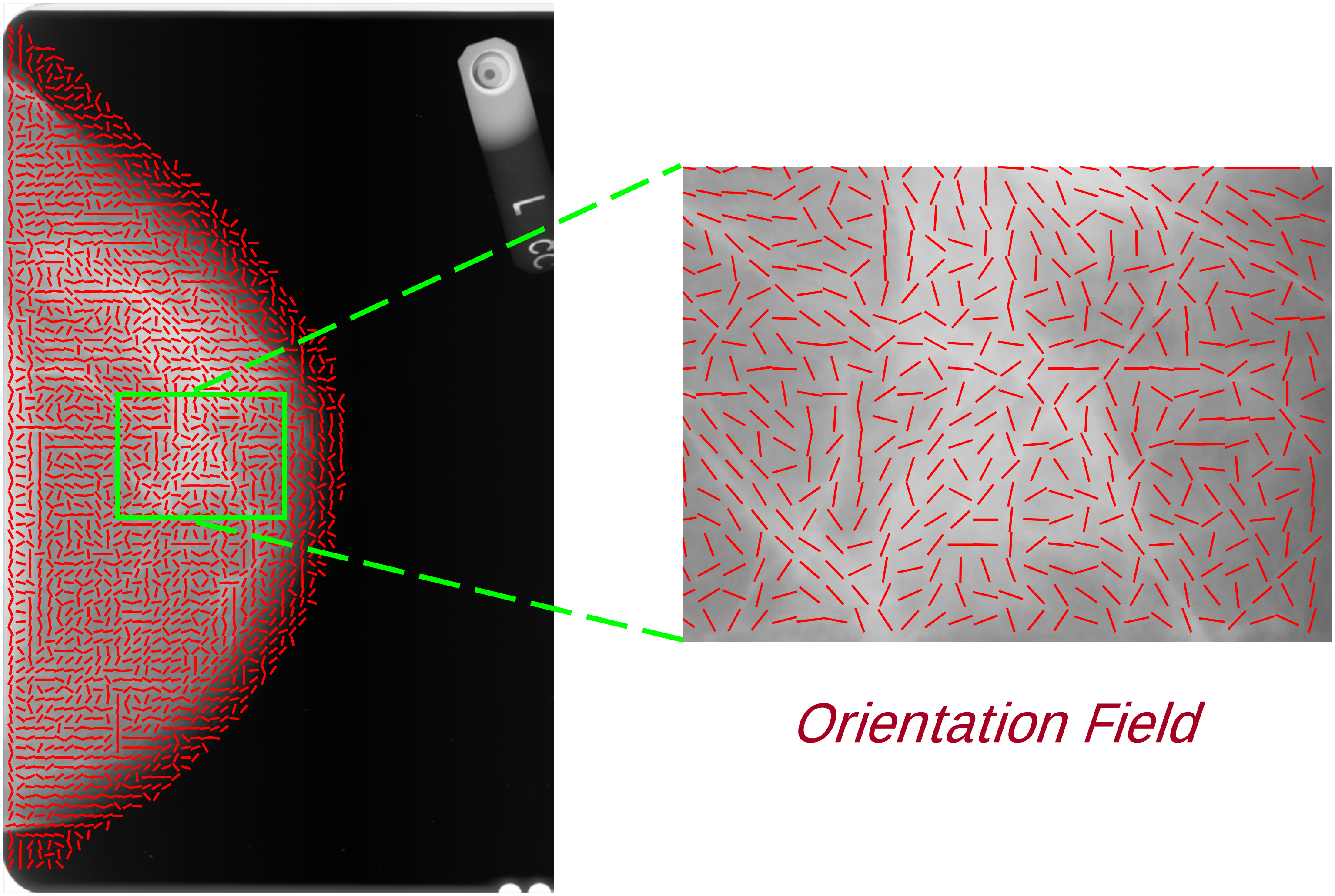

Orientation Field

Site of architectural distortion

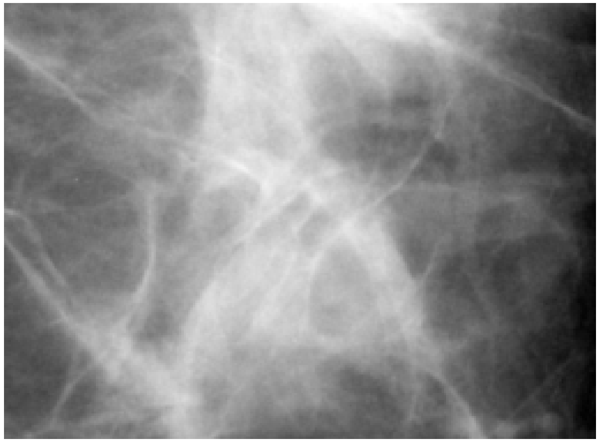

Mammogram

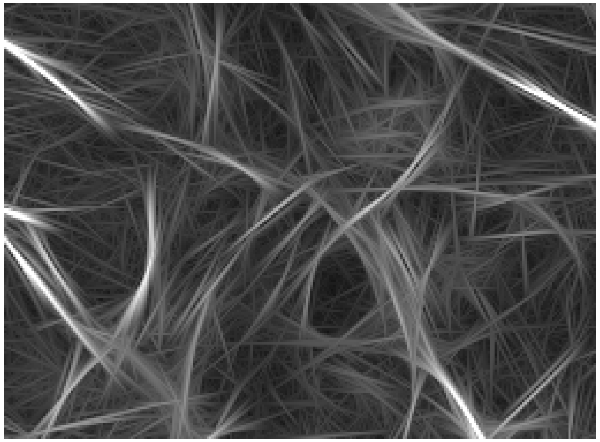

Gabor magnitude

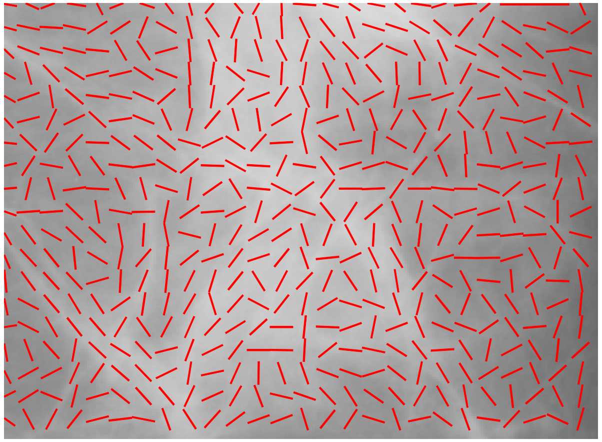

Orientation field

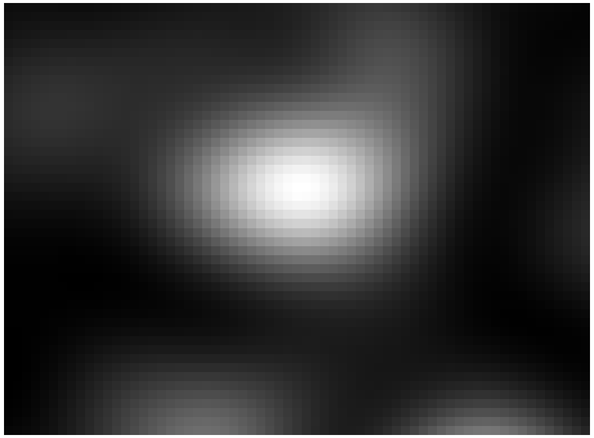

Node map

Interval cancer: potential sites of architectural distortion

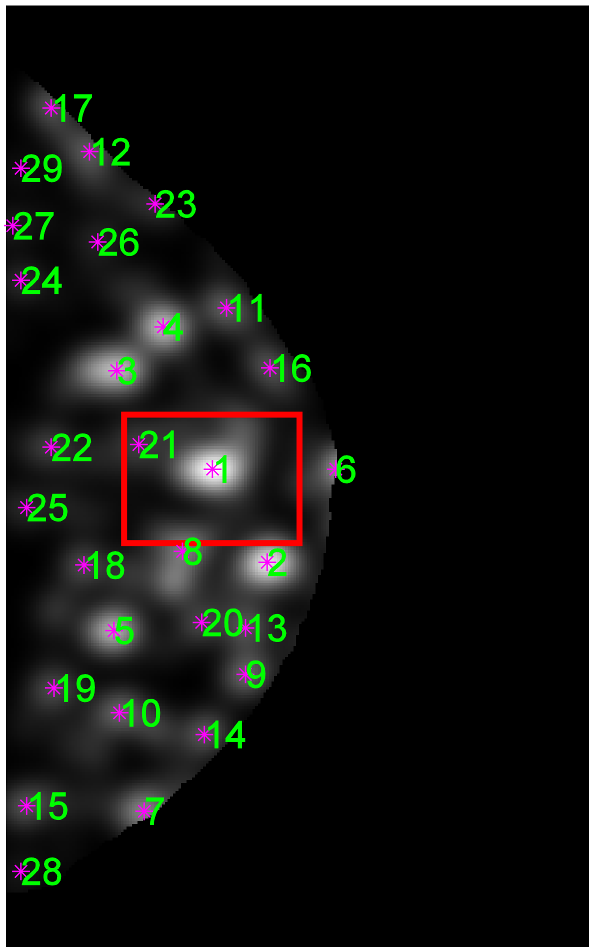

Node Map

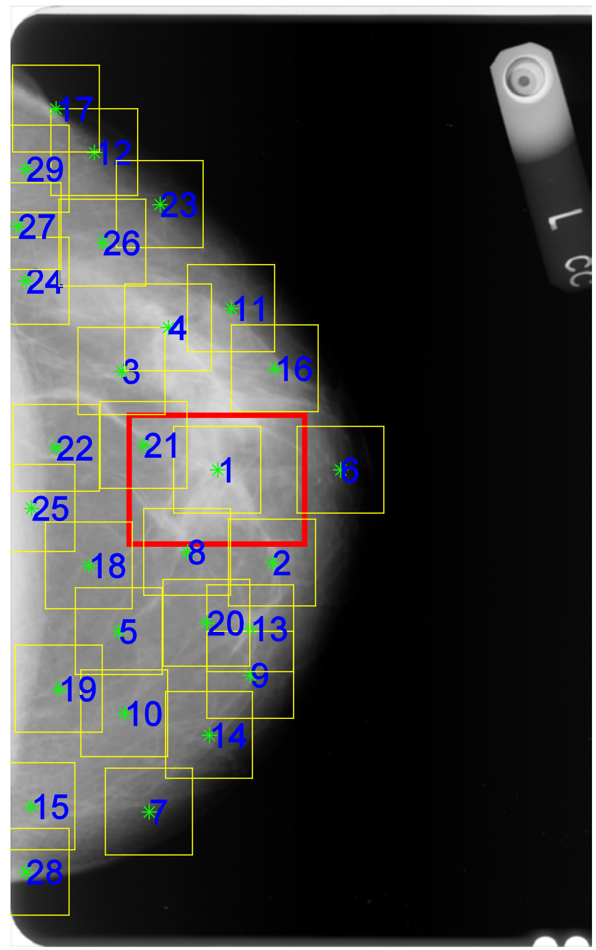

Automatically Detected ROIs

Examples of detected ROIs

True-positive

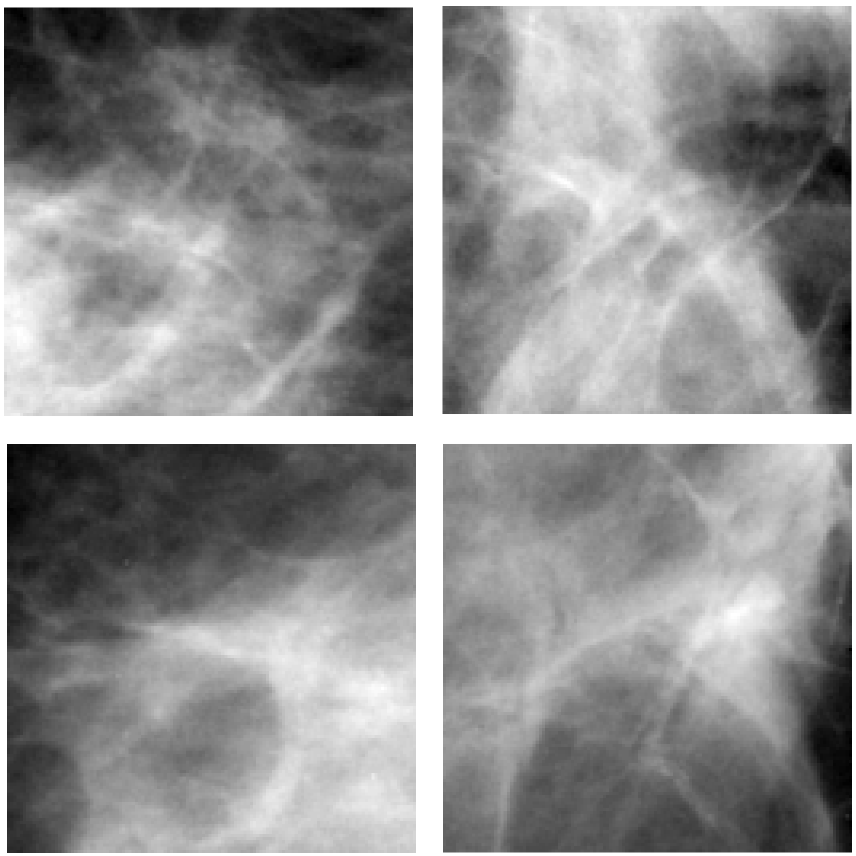

False-positive

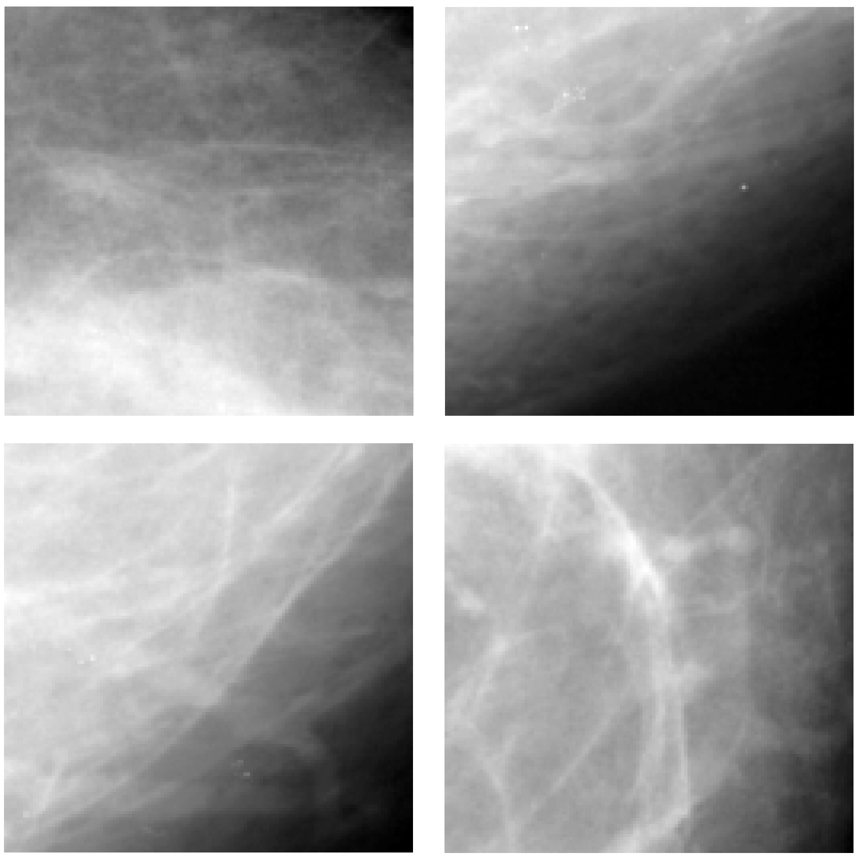

Automatically detected ROIs

Data Set	No. of Images	No. of ROIs 128 x 128 pixels at 200 µm/pixel	No. of True-Positive ROIs	No. of False-Positive ROIs
Prior mammograms of 56 interval-cancer cases	106	2821	301	2520
Prior mammograms of 13 normal cases	52	1403	0	1403
Total	158	4224	301	3923

Feature extraction from ROIs

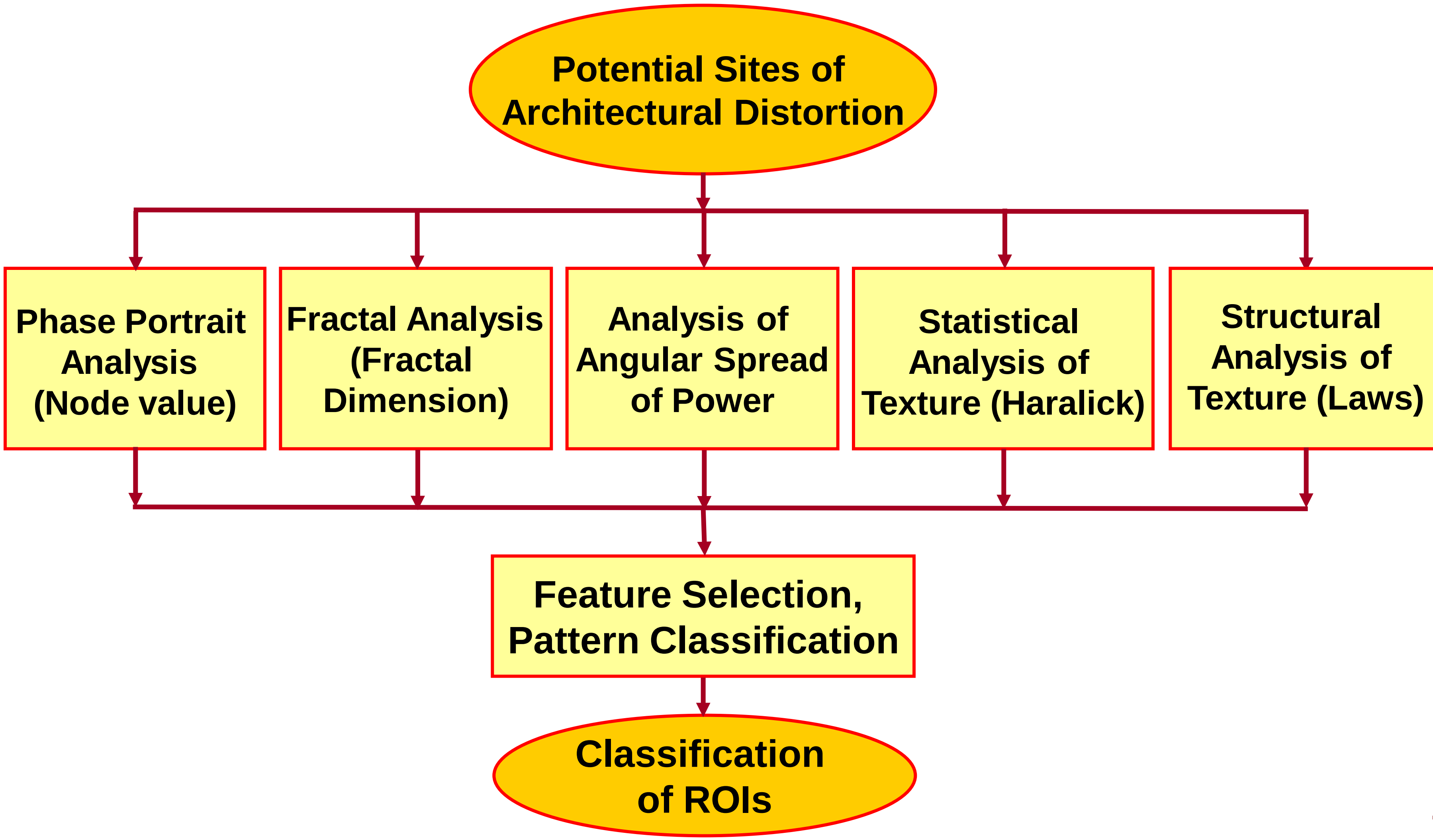

Fractal and spectral analysis

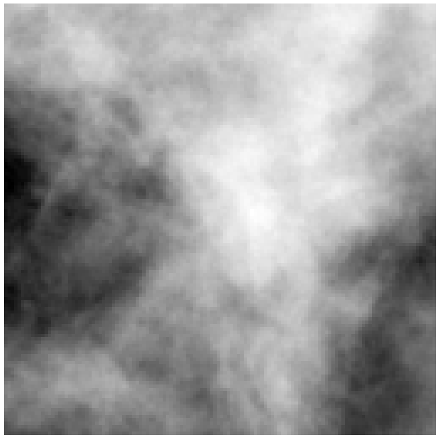

A TP ROI, $s(x, y)$

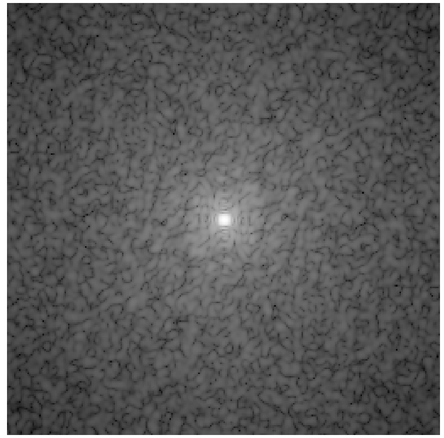

Fourier power spectrum, $S(u, v)$

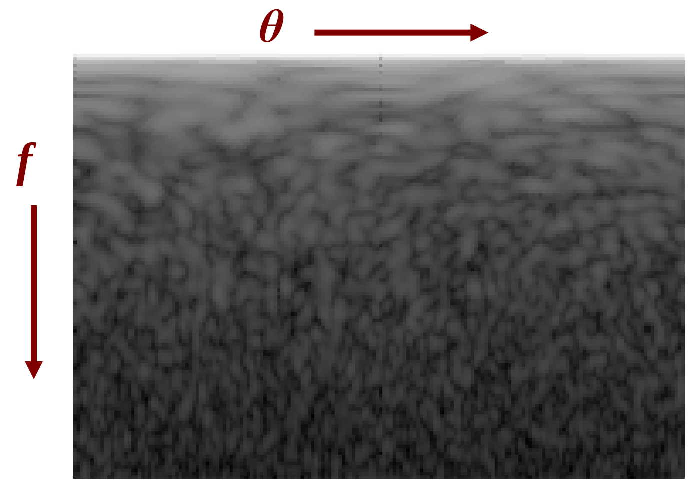

Power spectrum in polar coords, $S(f, \theta)$

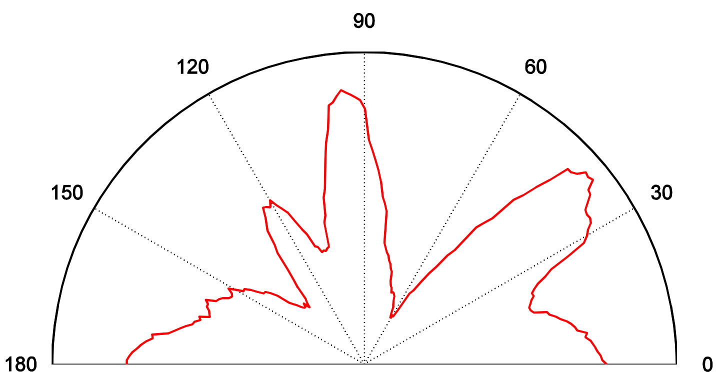

Angular spread of power, $S(\theta)$

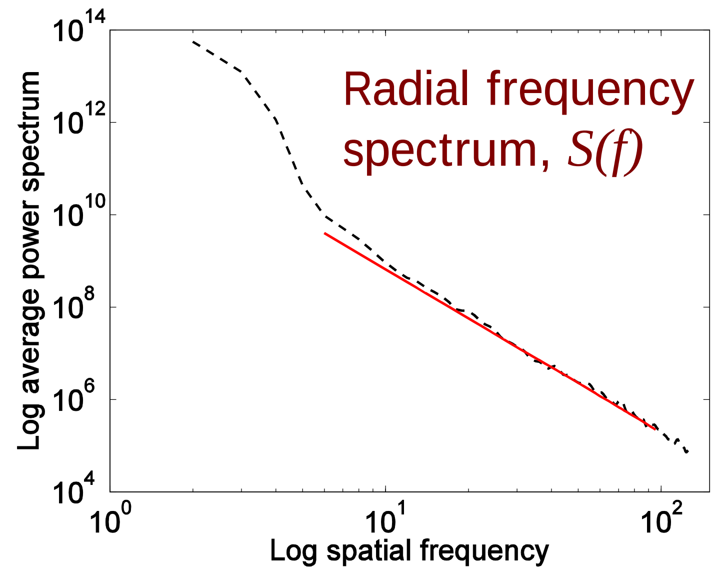

Radial frequency spectrum, $S(f)$

Laws' texture energy measures

- Operators of length five pixels may be generated by convolving the basic L3, E3, and S3 operators:
  - $L5 = L3 * L3 = [\ 1\ \ 4\ \ 6\ \ 4\ \ 1]$ (local average)
  - $E5 = L3 * E3 = [\ -1\ \ -2\ \ 0\ \ 2\ \ 1]$ (edges)
  - $S5 = -E3 * E3 = [\ -1\ \ 0\ \ 2\ \ 0\ \ -1]$ (spots)
  - $R5 = -S3 * S3 = [\ 1\ \ -4\ \ 6\ \ -4\ \ 1]$ (ripples)
  - $W5 = -E3 * S3 = [\ -1\ \ 2\ \ 0\ \ -2\ \ 1]$ (waves)
- 2D 5×5 convolution operators:
  - $L5L5 = L5^T L5$
  - $W5W5 = W5^T W5$
  - $R5R5 = R5^T R5$ etc.

Results of Laws' operators

L5L5

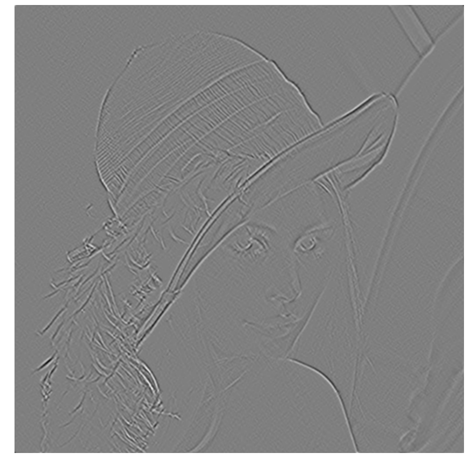

E5E5

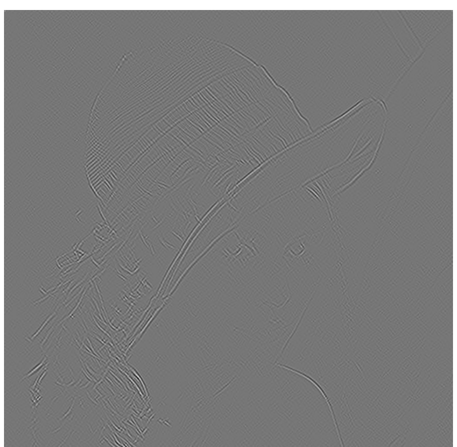

S5S5

W5W5

R5R5

Laws' texture energy

Sum of the absolute values in a 15×15 sliding window

L5L5

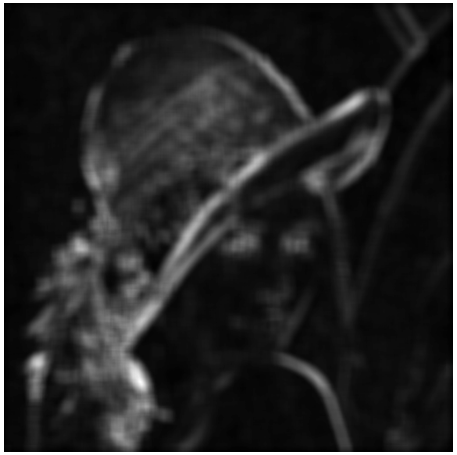

E5E5

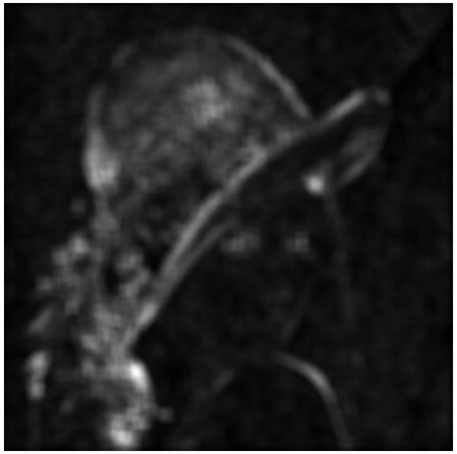

S5S5

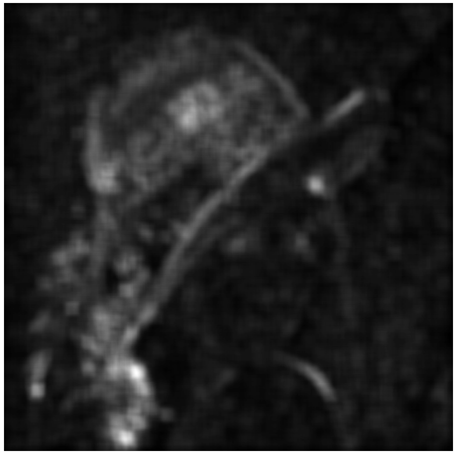

W5W5

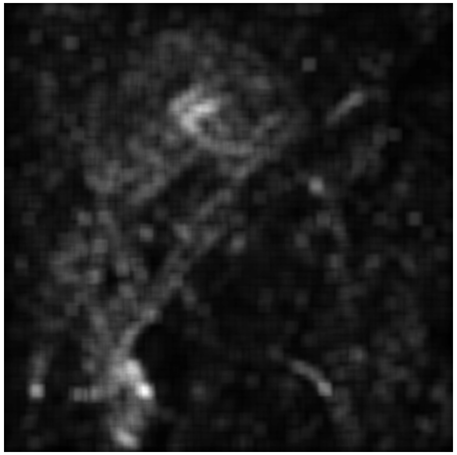

R5R5

Geometrical transformation for Laws' feature extraction

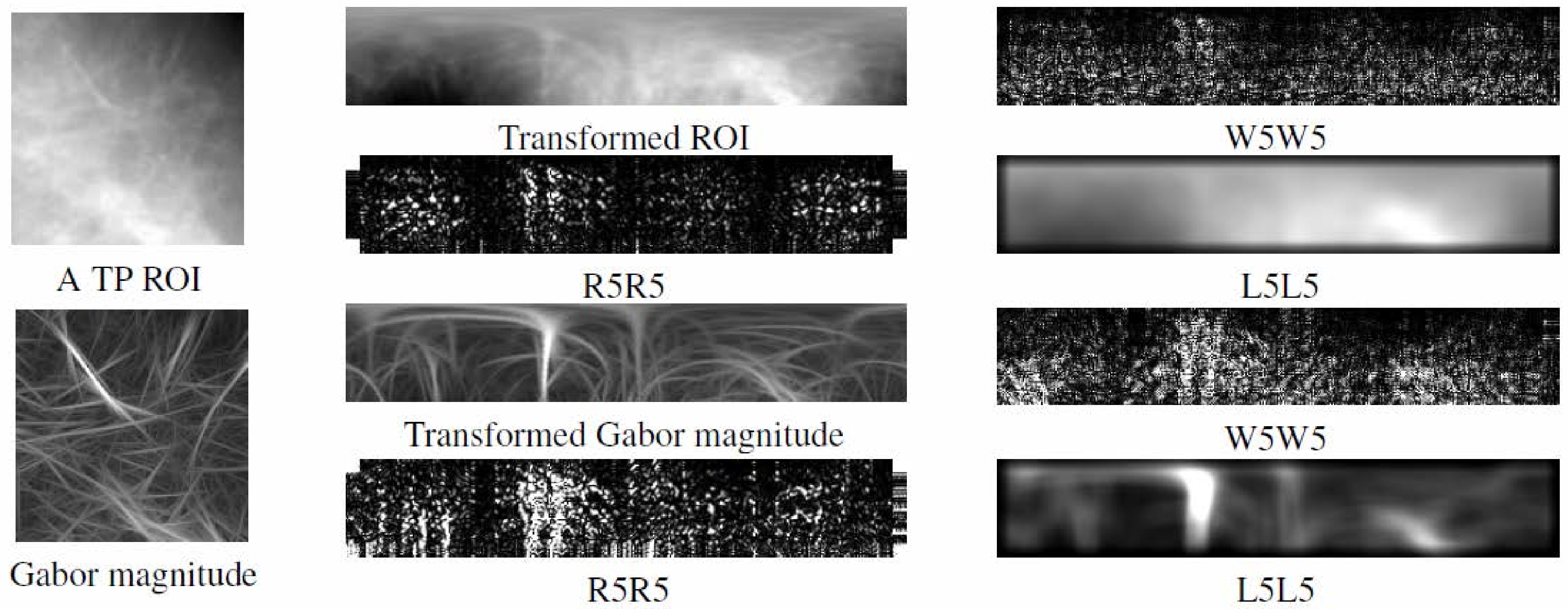

Analysis of angular spread: TP ROI

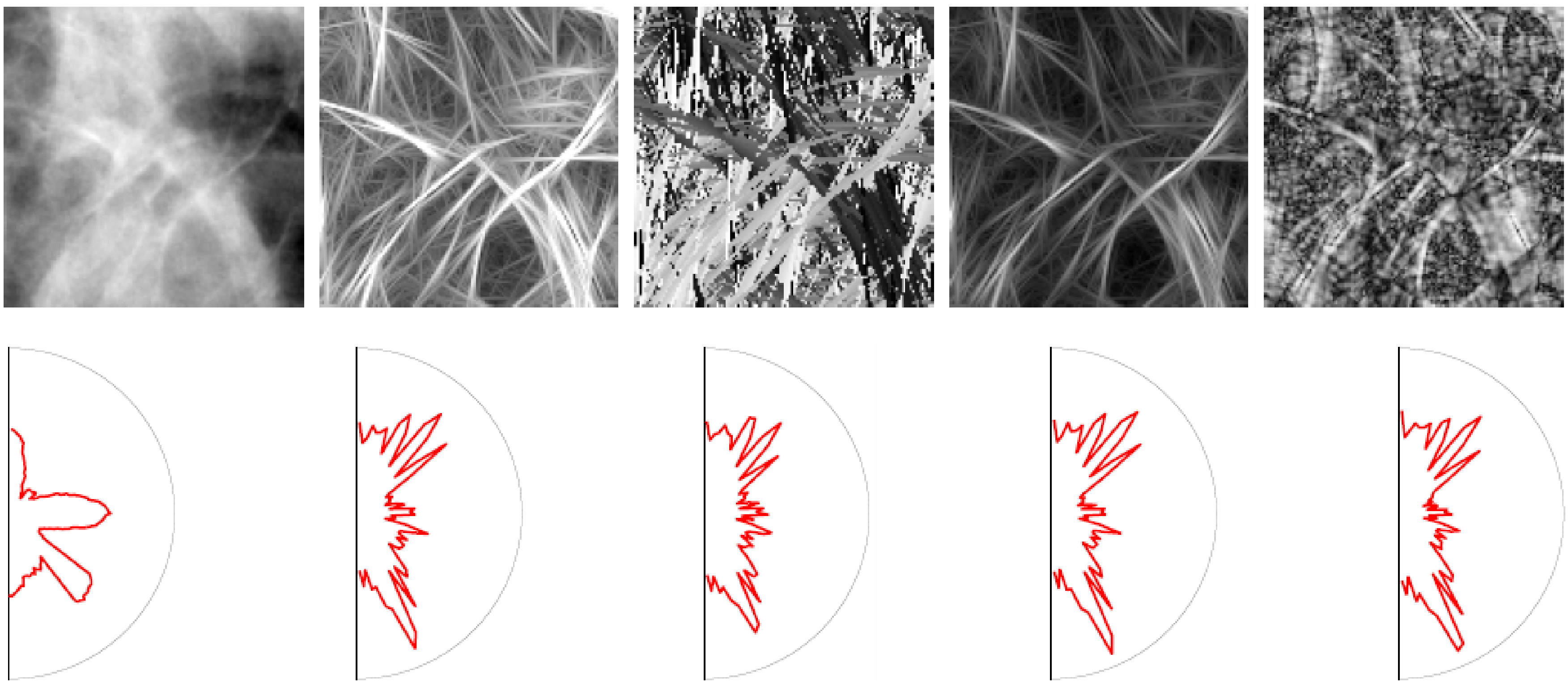

Frequency domain | Gabor magnitude | Gabor orientation | Coherence | Orientation strength

Analysis of angular spread: FP ROI

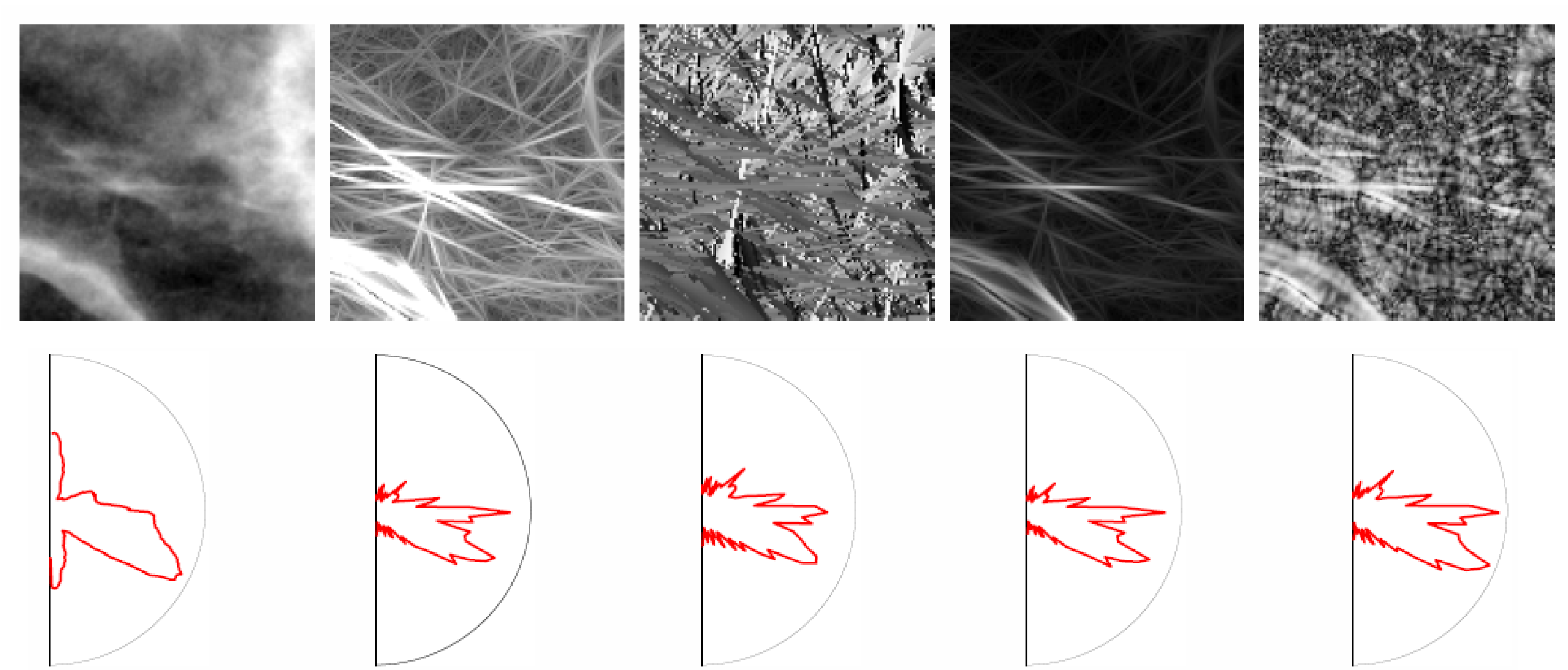

Frequency domain

Gabor magnitude

Gabor orientation

Coherence

Orientation strength

Receiver operating characteristics with selected features

Classifiers	AUC using the selected features with stepwise logistic regression
FLDA (Leave-one-ROI-out)	0.75
Bayesian (Leave-one-ROI-out)	0.76
SLFF-NN (Single-layer feed forward: tangent-sigmoid)	0.78
SLFF-NN* (Single-layer feed forward: tangent-sigmoid)	**0.78** ± 0.02

* 2-fold random subsampling, repeated 100 times

Free-response ROC (2011)

Sensitivity =

80% at 5.8 FP/image
90% at 8.1 FP/image

with the selected features based on stepwise logistic regression and using the Bayesian classifier and the leave-one-image out method

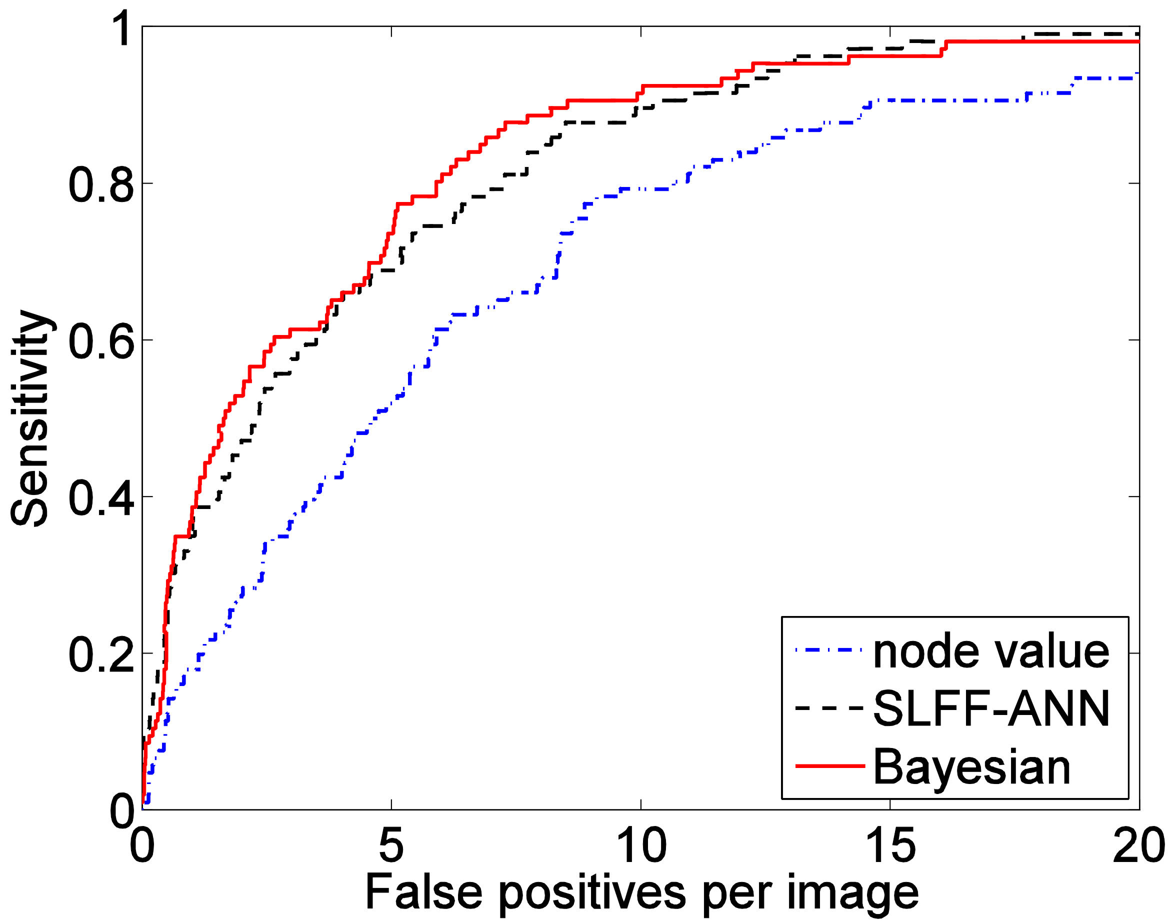

Bayesian ranking of ROIs: unsuccessful case

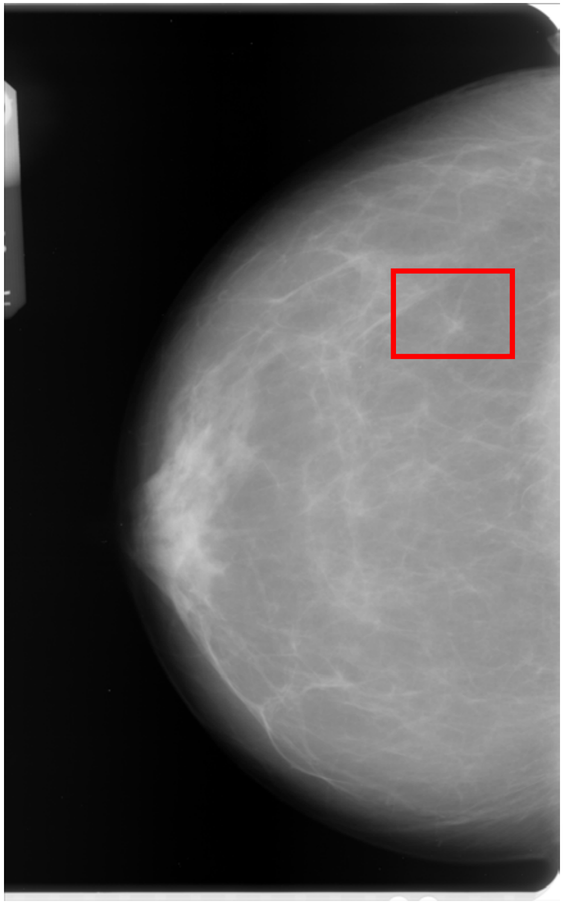

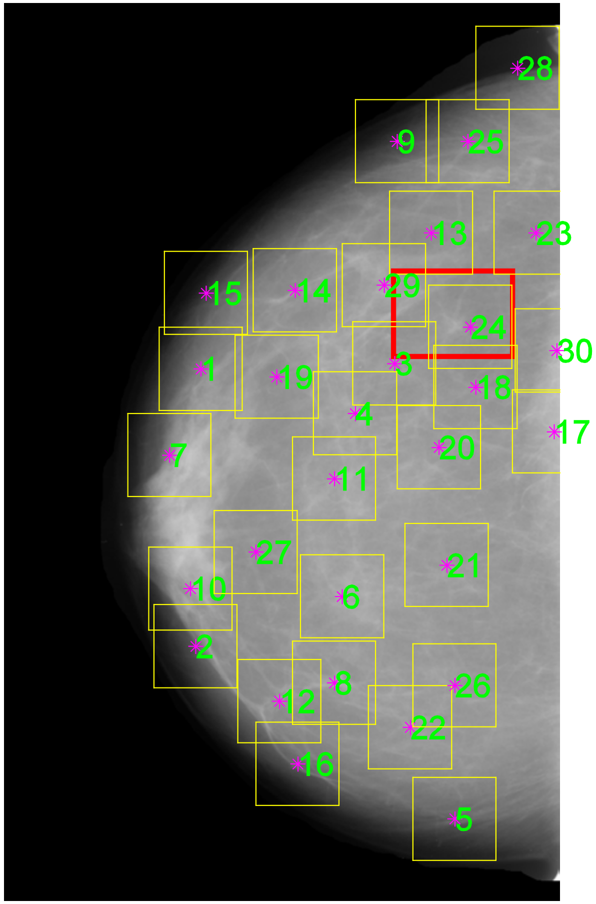

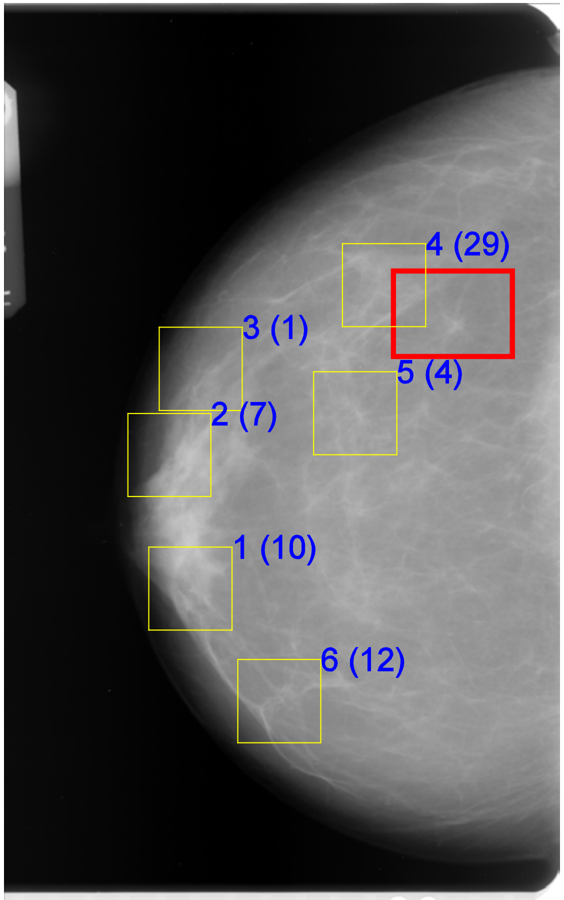

Bayesian ranking of ROIs: successful detection

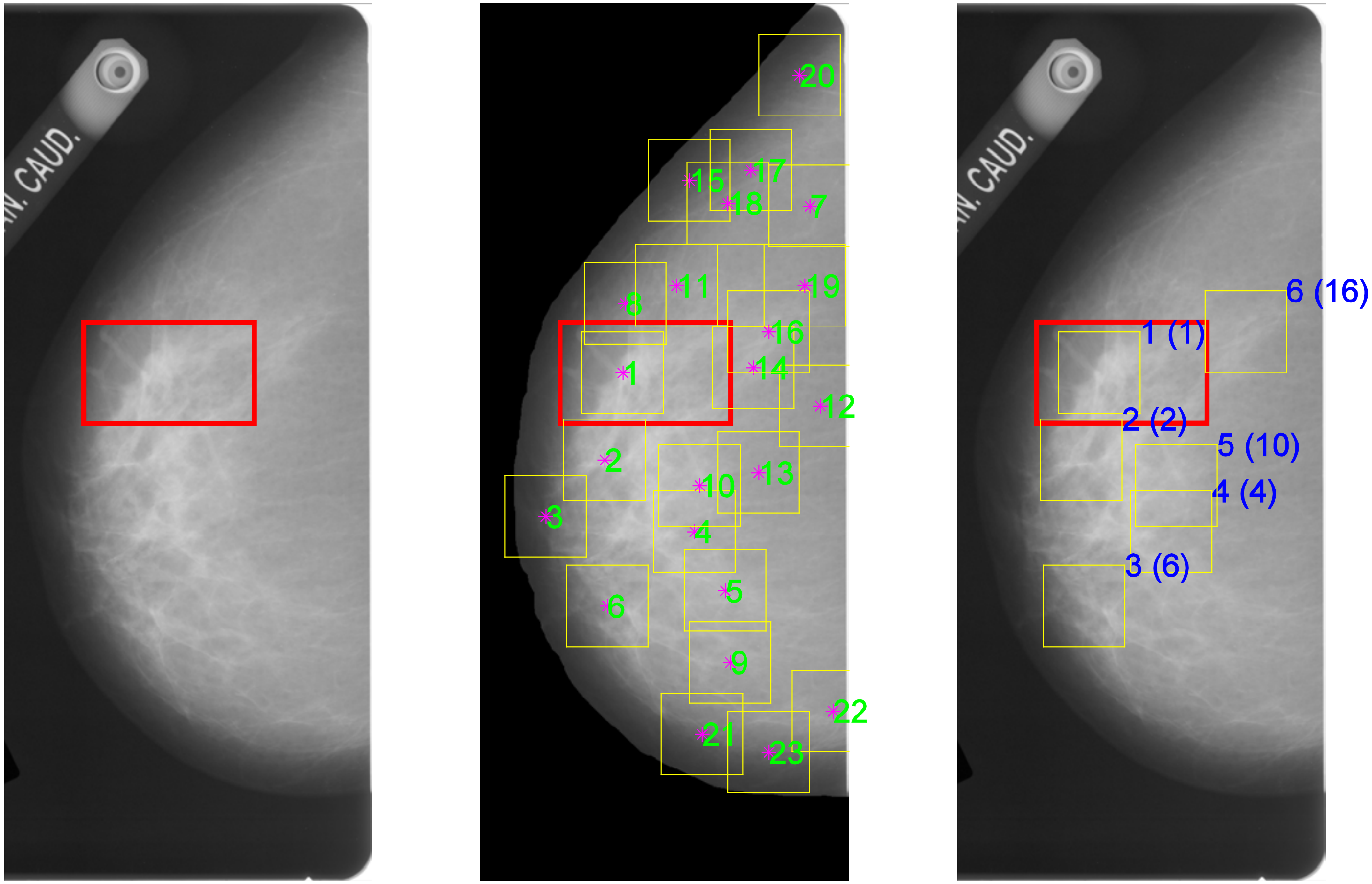

Characterization of Dispersion

The methods are based upon analysis of spicularity and angular dispersion caused by architectural distortion.

- Index of convergence of spicules (ICS)

$$\mathrm{ICS} = \sum_{i=1}^{P}\sum_{j=1}^{Q} M(i,j)\left|\cos[\theta(i,j) - \alpha(i,j)]\right|$$

$P \times Q$: size of the ROI

$\theta(i, j)$: Gabor angle response within the range [-89°, 90°]

$M(i, j)$: Gabor magnitude or coherence value

$\alpha(i, j)$: angle of a pixel with respect to the horizontal toward the center of ROI, in the range [-89°, 90°]

Index of Convergence of Spicules

ICS quantifies the degree of alignment of each pixel toward the center of the ROI weighted by the Gabor magnitude or coherence value.

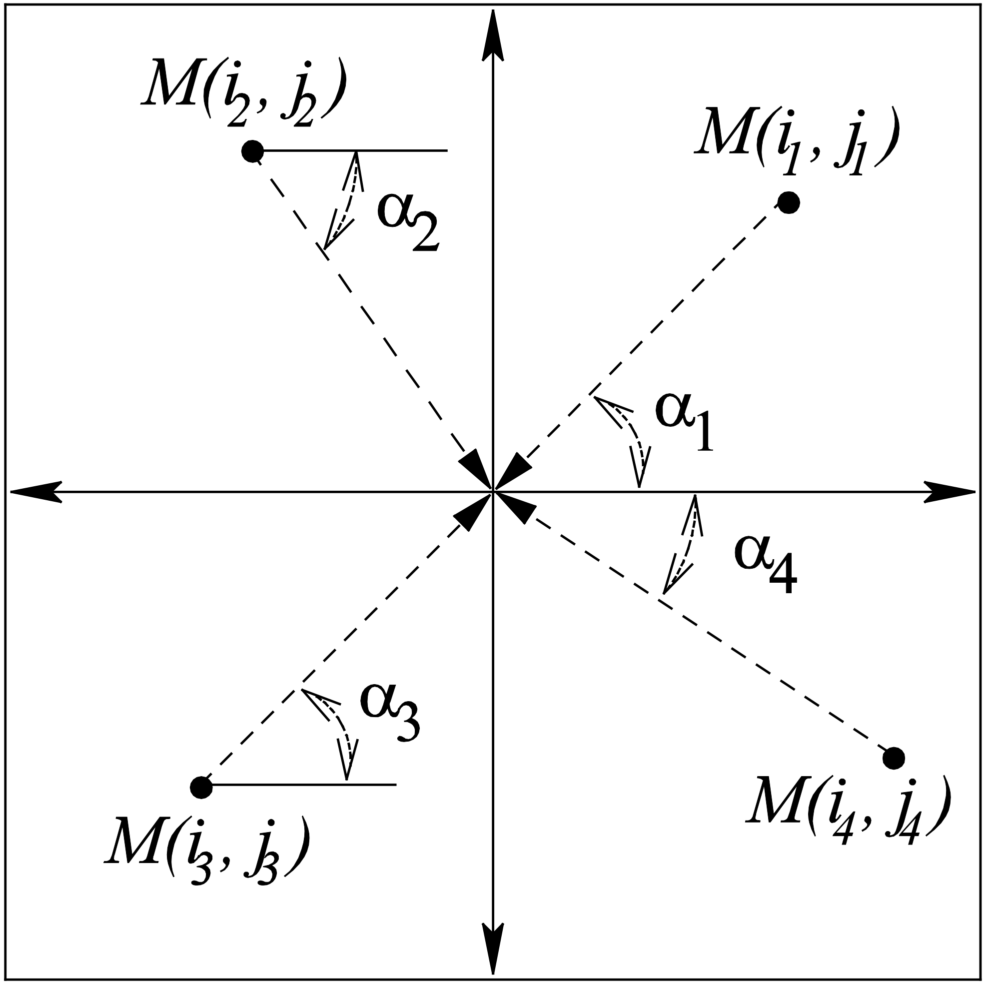

Radially Weighted Difference

$$\mathrm{RWD} = \sum_{p=1}^{PQ} \sum_{q=1}^{PQ} |I_p - I_q||r_p - r_q|$$

I: attribute value (intensity or magnitude)

r: radial distance from the center of the ROI

$\alpha(i, j)$: angle of a pixel with respect to the horizontal toward the center of ROI, in the range $[0°, 359°]$

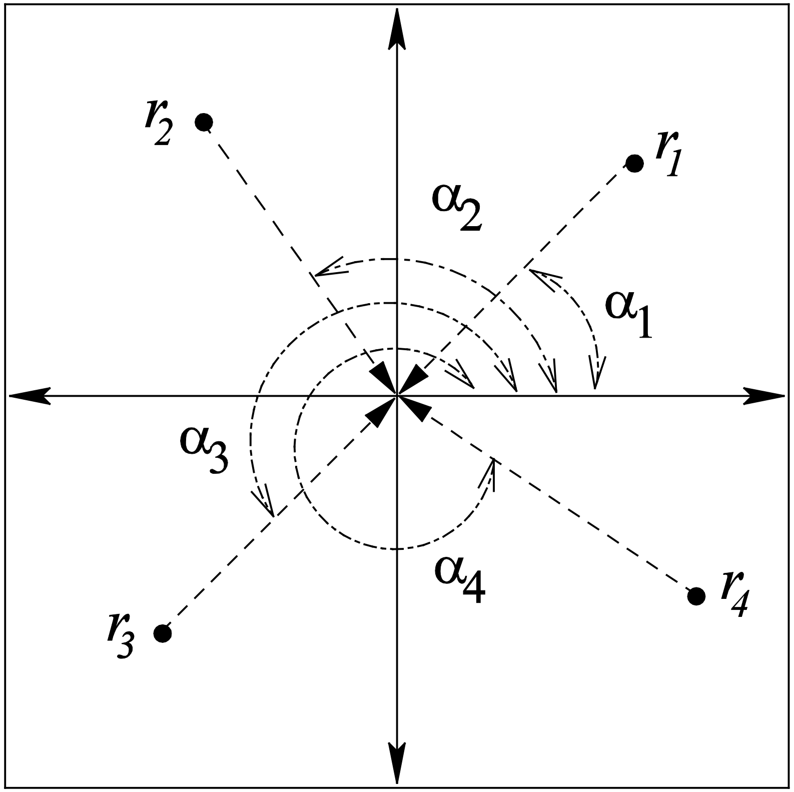

Angle Weighted Difference

$$\text{AWD} = \sum_{p=1}^{PQ} \sum_{q=1}^{PQ} |I_p - I_q| |\sin(|\alpha_p - \alpha_q|)|$$

I: attribute value (intensity or magnitude)

r: radial distance from the center of the ROI

$\alpha(i, j)$: angle of a pixel with respect to the horizontal toward the center of ROI, in the range $[0°, 359°]$

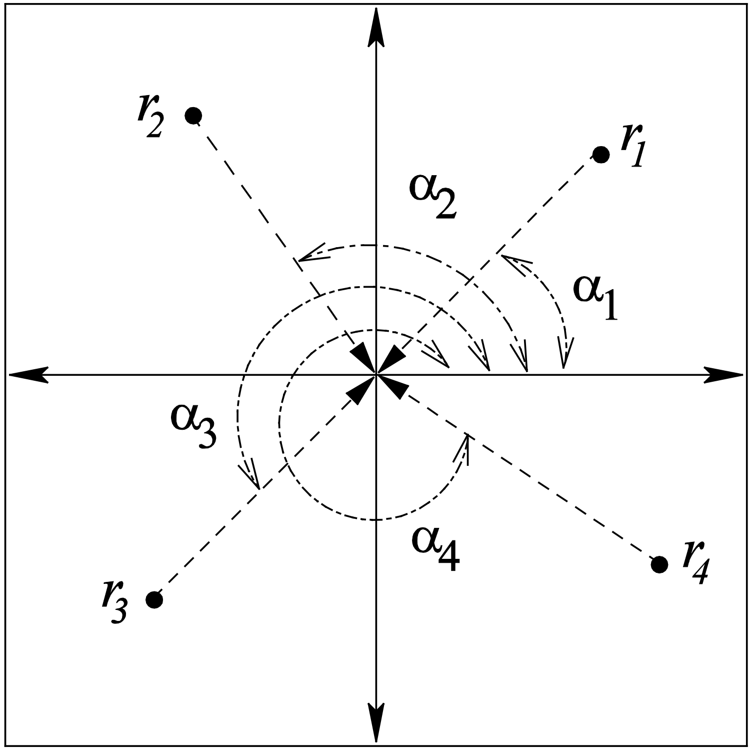

Angle-weighted Difference in the Entropy of Spicules

$$\mathrm{AWDES} = \sum_{m=1}^{90} \sum_{n=1}^{90} |H_m - H_n| |\sin(|\alpha_m - \alpha_n|)|$$

α: angular bands or sectors with their angles with respect to the x-axis toward the center of ROI (with 90 bins over [0°, 359°])

H: entropy of the attributes (intensity, magnitude, or angle) in the angular bands

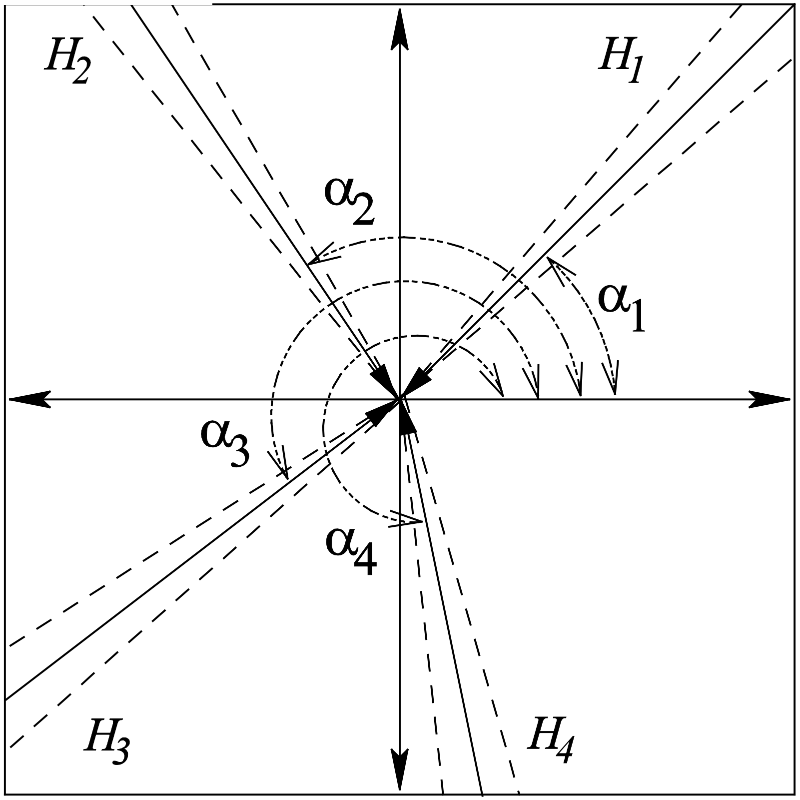

ROC Performance of Features

Feature symbol	Feature name	A_z value
Node	Node value	0.61
ICS_m	ICS of magnitude	0.65
ICS_c	ICS of coherence	0.64
RWD_i	RWD of intensity	0.53
RWD_m	RWD of magnitude	0.62
RWD_a	RWD of angle	0.64
AWD_i	AWD of intensity	0.53
AWD_m	AWD of magnitude	0.62
AWD_a	AWD of angle	0.64
AWDES_i	AWDES of intensity	0.63
AWDES_m	AWDES of magnitude	0.64
AWDES_a	AWDES of angle	0.53

Performance of Combinations of Features

Feature Set	ROC Analysis (A_z)	FROC Analysis: Bayesian (FP/patient at sensitivities shown) 80%	90%
Node	0.61	8.2	13.9
All	0.73 (ANN-RBF)	5.7	8.1
Selected set: *RWDi*, *RWDm*, *RWDa*, *AWDi*, *AWDm*, *AWDa*, *AWDESm*	0.76 (ANN-RBF)	**5.3**	**6.3**

ANN-RBF: Artificial neural network based on radial basis functions

FROC Analysis (2012)

Sensitivity = 80%
at 5.3 FP/patient

Sensitivity = 90%
at 6.3 FP/patient

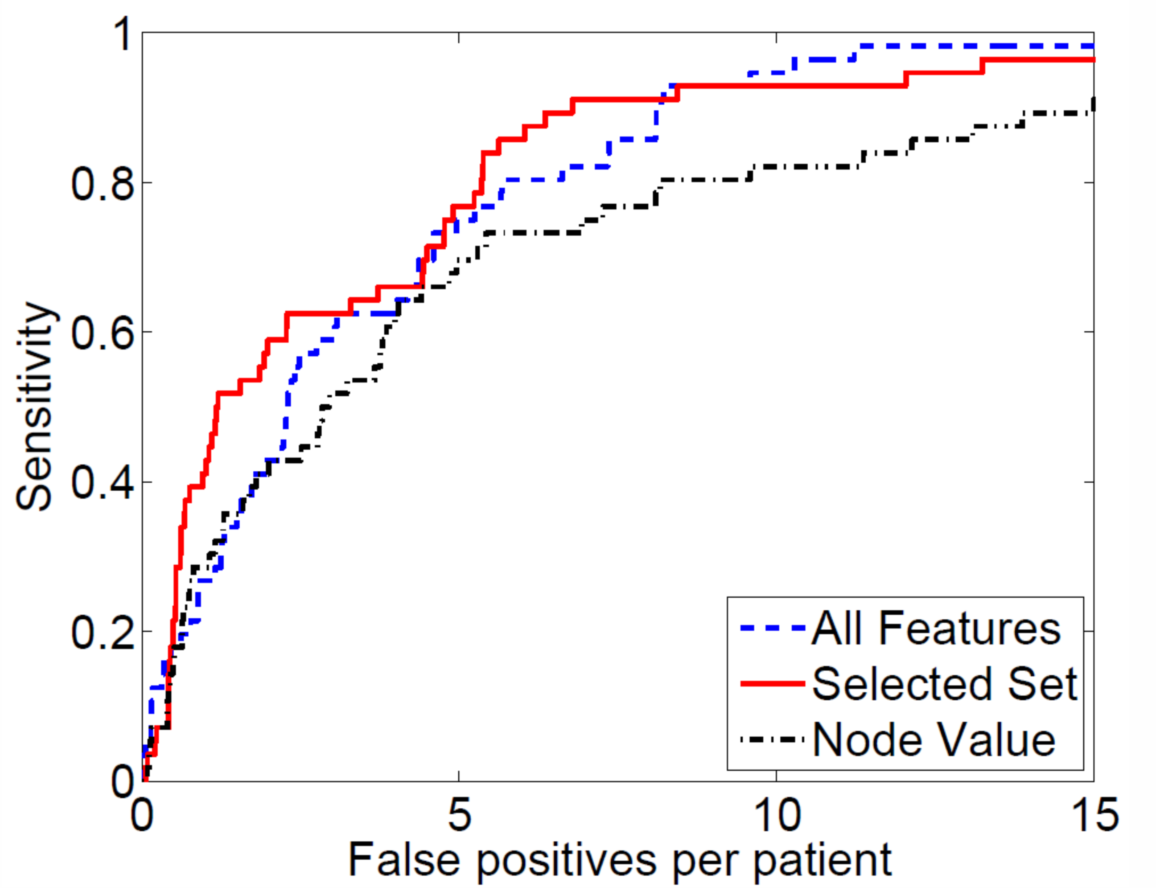

Other Approaches to Detect Architectural Distortion

Karssemeijer and te Brake, IEEE TMI 1996: multiscale-based method using the output of three-directional, second-order, Gaussian derivative operators

Sampat et al., IEEE SW Symp. Im. An. Int. 2006: linear filtering of the Radon transform of the given image for the enhancement of spicules; the enhanced image was filtered with radial spiculation filters

Other Approaches to Detect Architectural Distortion

Matsubara et al., CARS 2003, 2004: detection of architectural distortion near the skin line

Nemoto et al., *IJCARS 2009:* lines corresponding to spiculation of architectural distortion differ in characteristics from lines in the normal mammary gland; modified point convergence index weighted by the likelihood of spiculation calculated to enhance architectural distortion

Analysis of Spicules

Fig. 7 Extracted *lines* with likelihood of spiculation. *Lines* with high likelihood are displayed in *red* and those with low likelihood are drawn in *white*

Nemoto et al. IJCARS 2009

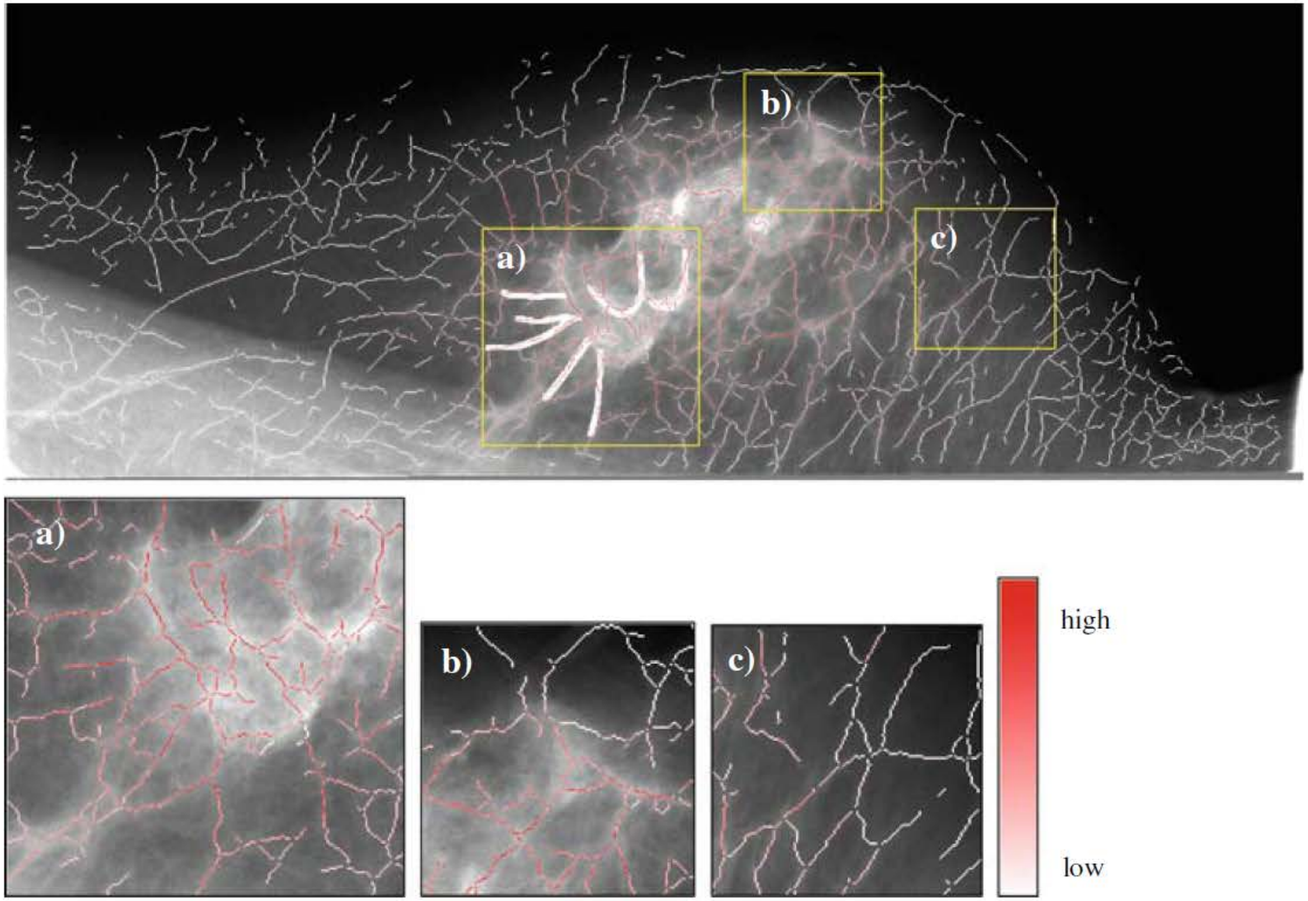

Fractal Analysis

Guo et al. IJCARS 2009: fractional Brownian motion model; regions with masses and architectural distortion have lower fractal dimension and higher lacunarity than normal regions

Tourassi et al. Phys. Med. Biol. 2006: fractal dimension using power spectral analysis

Rangayyan et al. IJCARS 2007: fractal analysis and texture analysis of ROIs detected in prior mammograms of cases of screen-detected cancer

Expected Loci of Breast Tissue

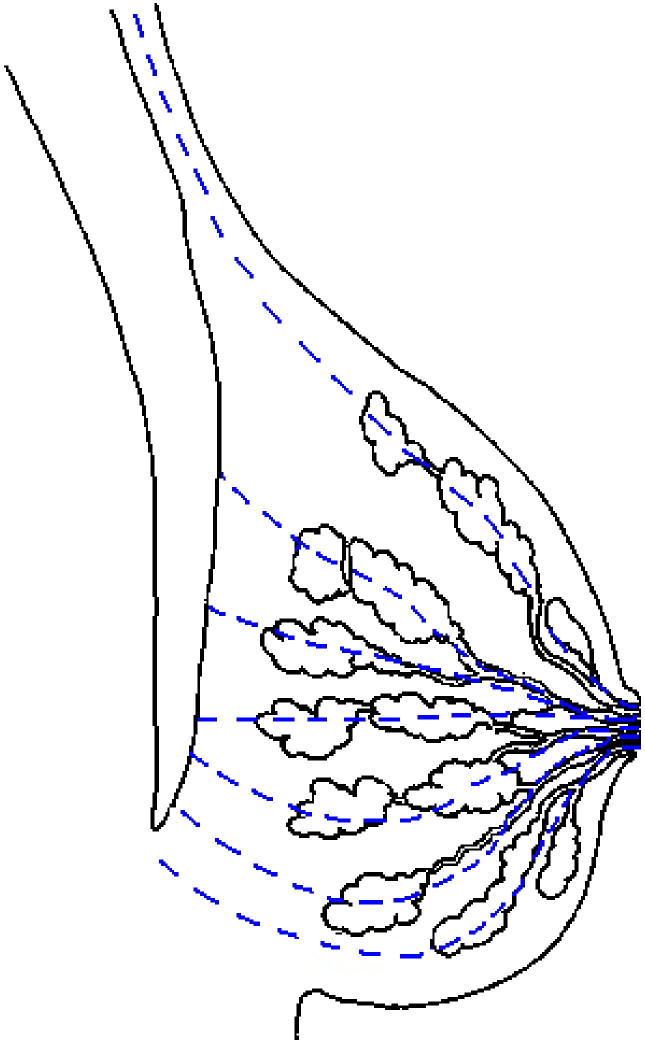

CBMS 2012,
IJCARS 2012

Landmarking of Mammograms:
Breast Boundary, Pectoral Muscle, Nipple

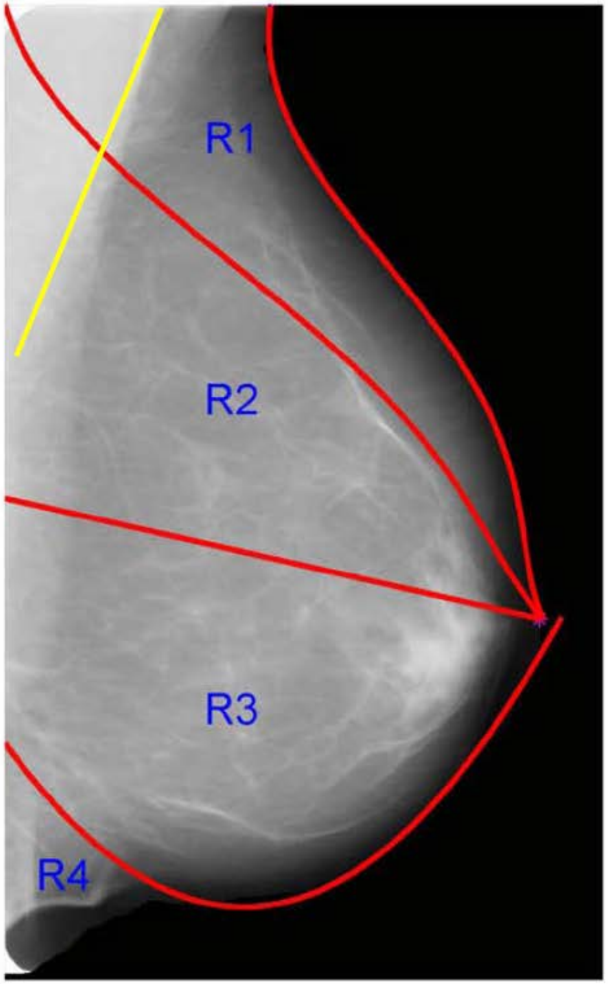

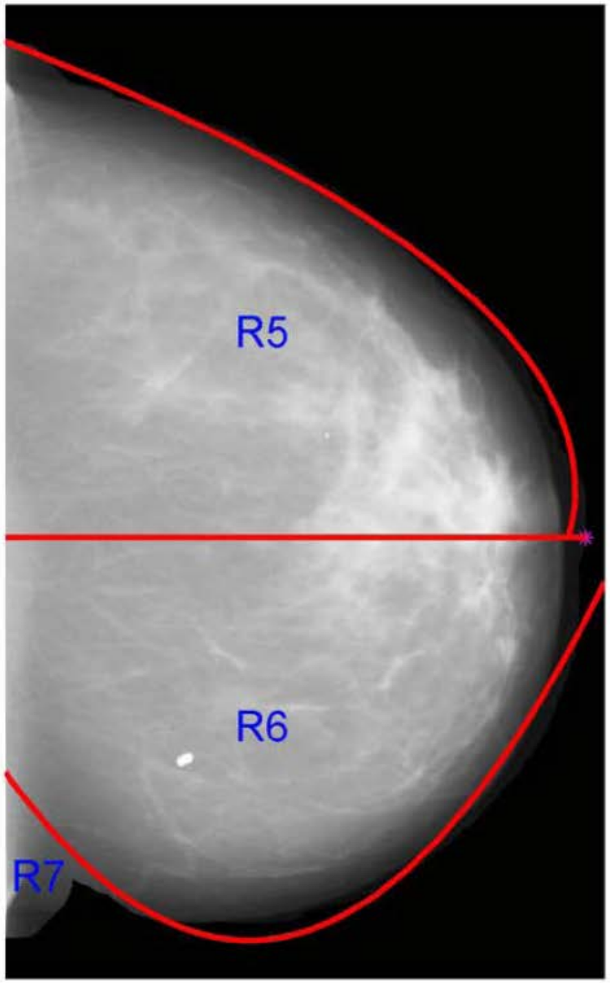

Second- and fifth-order polynomials fitted to parts of breast boundary

Derivation of Expected Loci of Breast Tissue: Interpolation

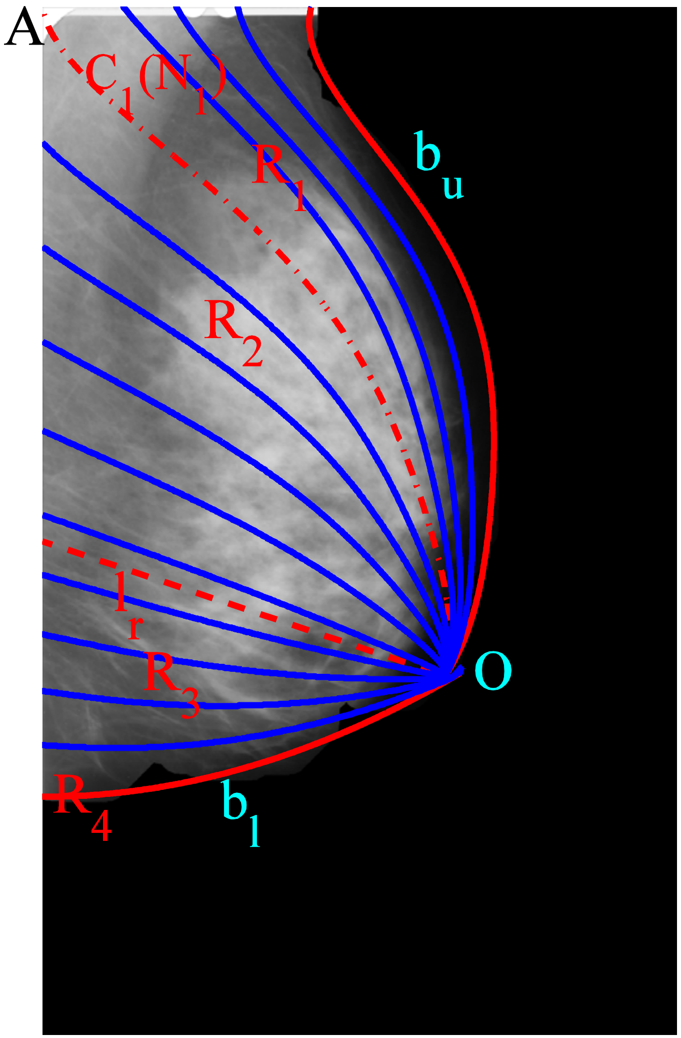

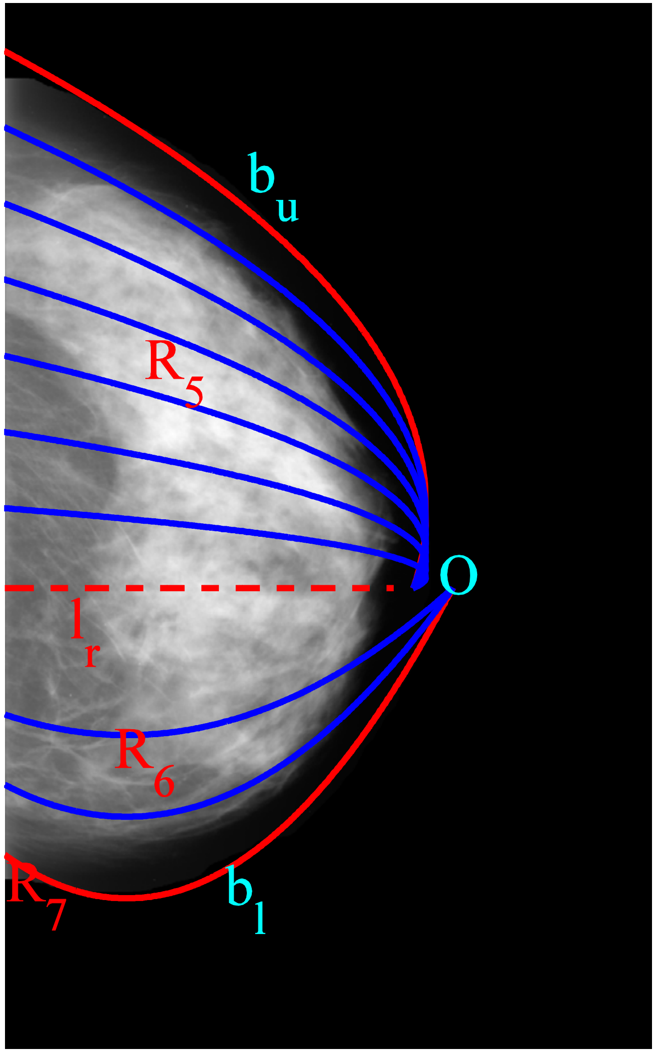

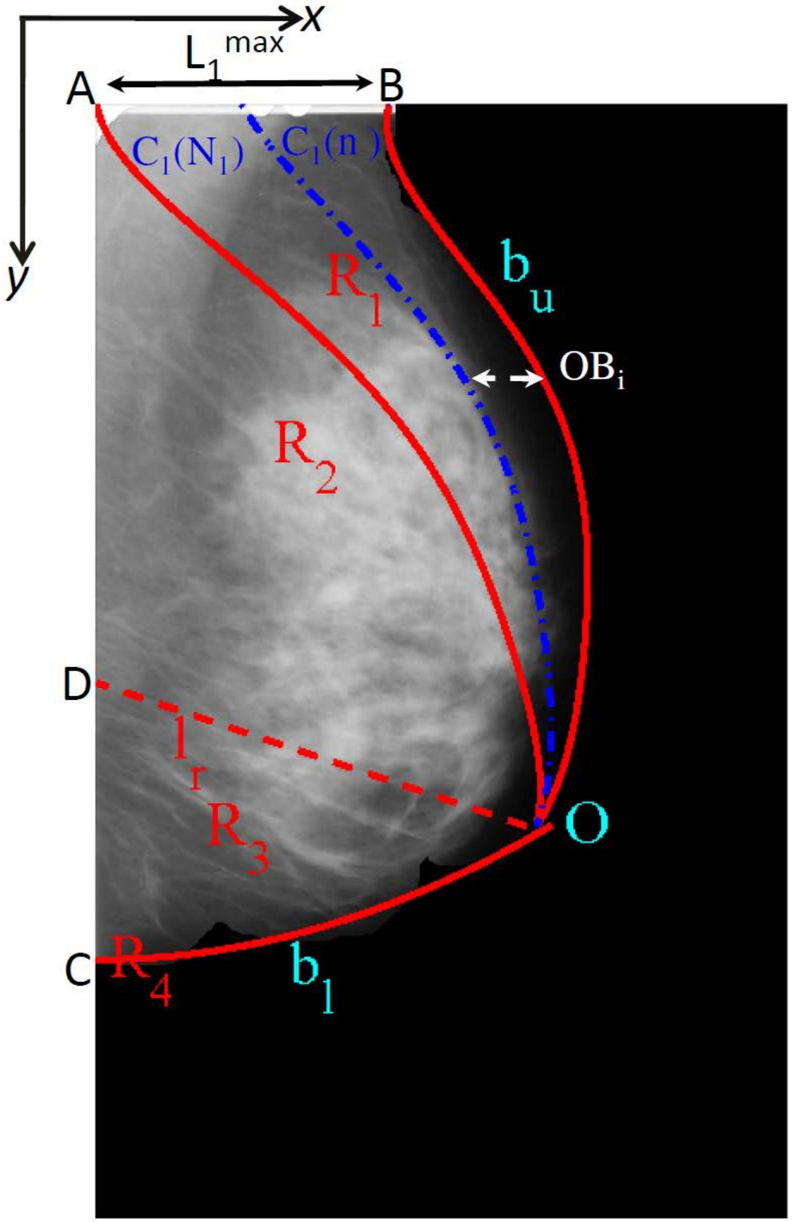

Distance between curves decreases with equal steps from AB to O

Number of curves = N_1 ; L_1^{max} = N_1 -1

Distance between curves = 1 at AB

All curves contain M_1 points

Decrement along y-axis = $1/M_1$

i-th point of n-th curve:

$$x_i(n) = x_i(1) - \left(\frac{n-1}{M_1 - 1}\right)[i-1]$$

$$y_i(n) = y_i(1)$$

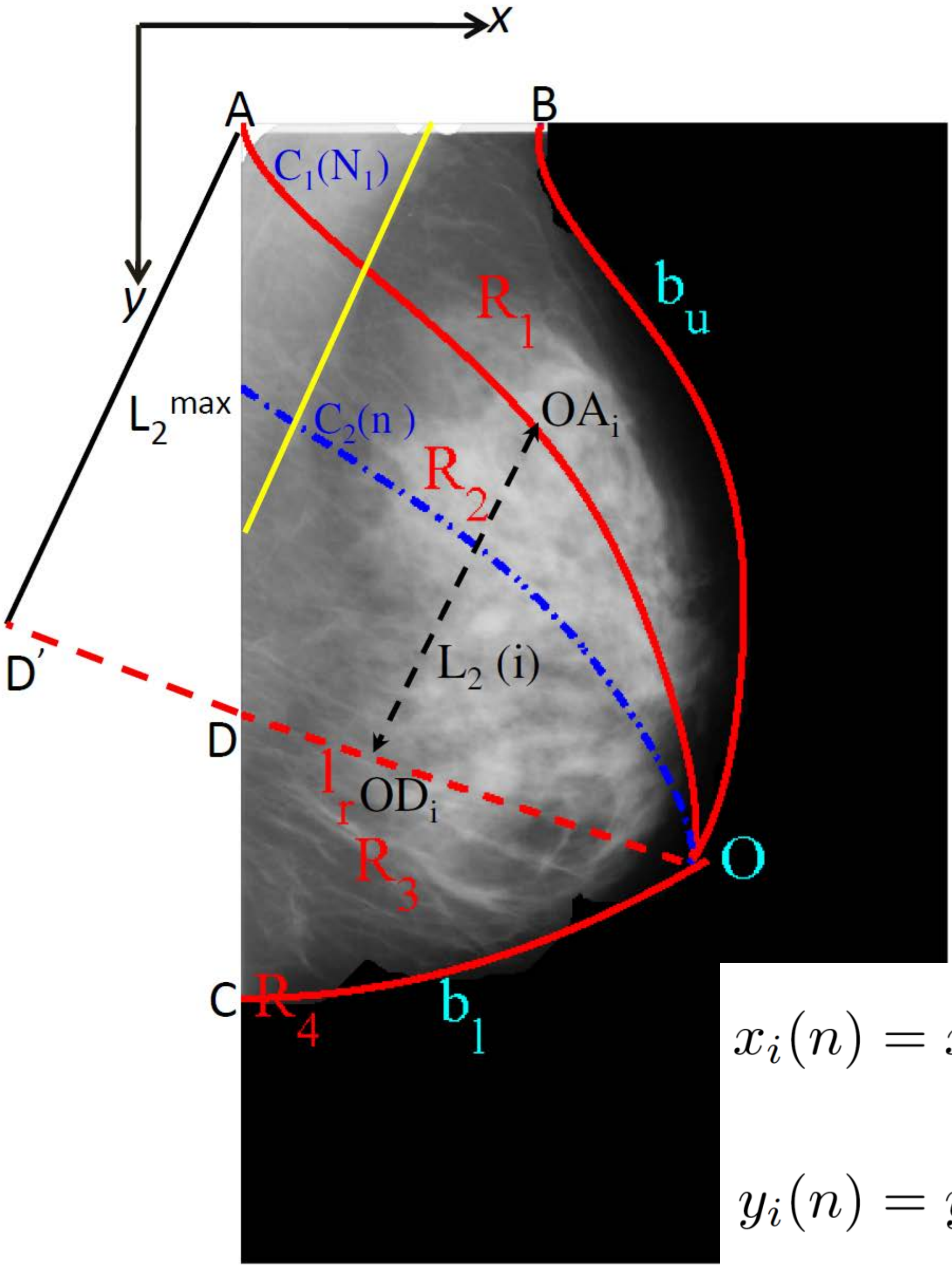

Number of points in curve = M

L_i = ⊥ length between two curves at the i-th point

$L_{max} = max(L_i)$

Number of curves = N = L_{max}+1

Distance at i-th point = L_i / L_{max} = $L_i / (N-1)$

i-th point of n-th curve:

$$x_i(n) = x_i(1) - [x_i(1) - x_i(N_2)]\left(\frac{n-1}{N_2-1}\right)$$

$$y_i(n) = y_i(1) - [y_i(1) - y_i(N_2)]\left(\frac{n-1}{N_2-1}\right)$$

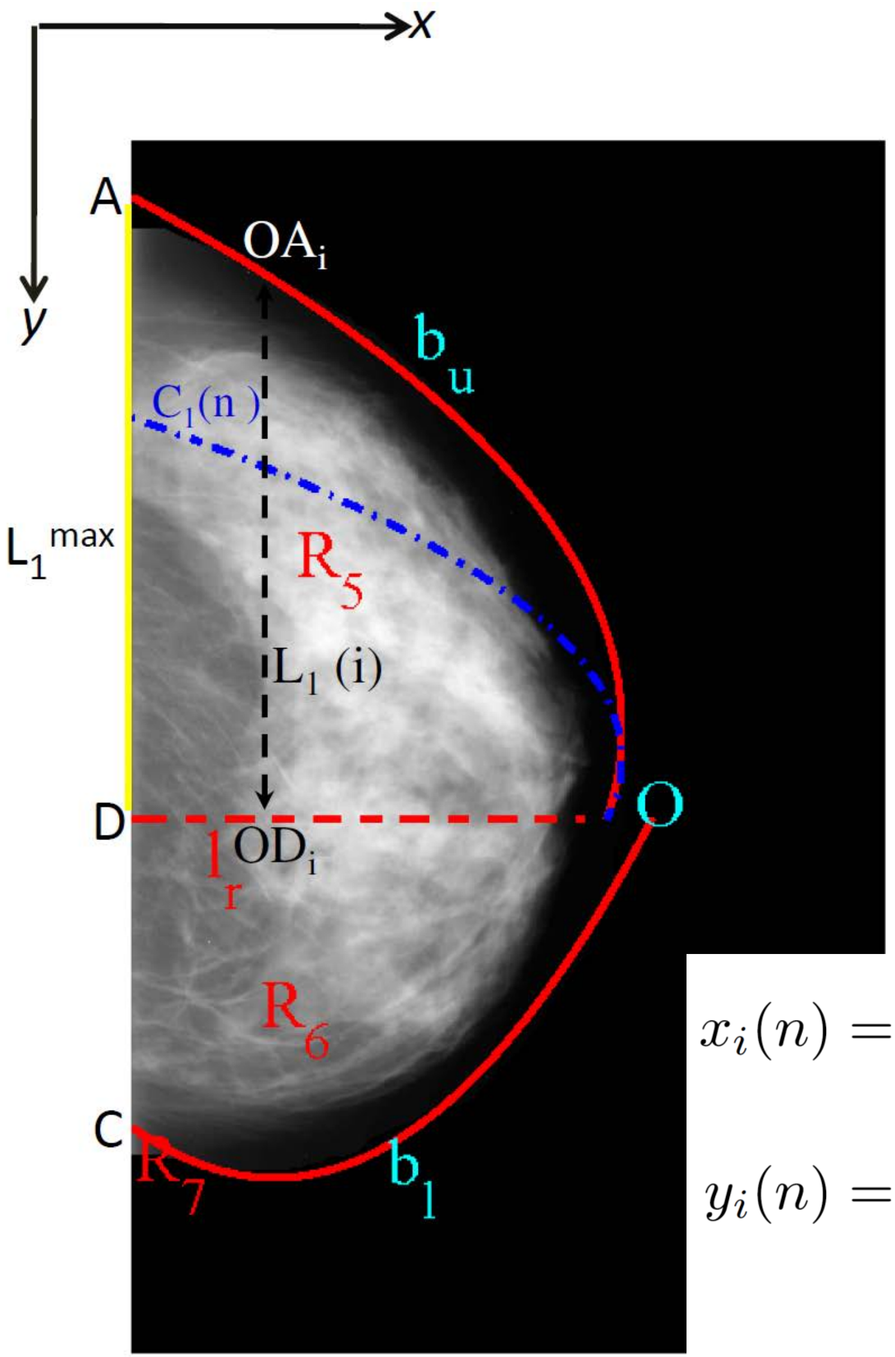

Number of points in curve = M

L_i = ⊥ length between two curves at the i-th point

$L_{max} = max(L_i)$

Number of curves = N = $L_{max}+1$

Distance at i-th point = L_i / L_{max} $= L_i / (N-1)$

i-th point of n-th curve:

$$x_i(n) = x_i(1) - [x_i(1) - x_i(N_2)] \left(\frac{n-1}{N_2 - 1} \right)$$

$$y_i(n) = y_i(1) - [y_i(1) - y_i(N_2)] \left(\frac{n-1}{N_2 - 1} \right)$$

Divergence with Respect to the Expected Loci of Breast Tissue

$$\gamma(i,j) = \frac{\sum_{m=1}^{L}\sum_{n=1}^{L} |M(m,n)\cos[\theta(m,n) - \phi(i,j)]|}{\sum_{m=1}^{L}\sum_{n=1}^{L} M(m,n)}$$

M: Gabor filter magnitude response
θ: Gabor filter angle response
ϕ: expected orientation of breast tissue
L: 25 pixels at 200 µm/pixel
180 Gabor filters used over [-90, 90] degrees

$$D(i,j) = 1 - \gamma(i,j)$$

Orientation Field of Breast Tissue Obtained Using Gabor Filters

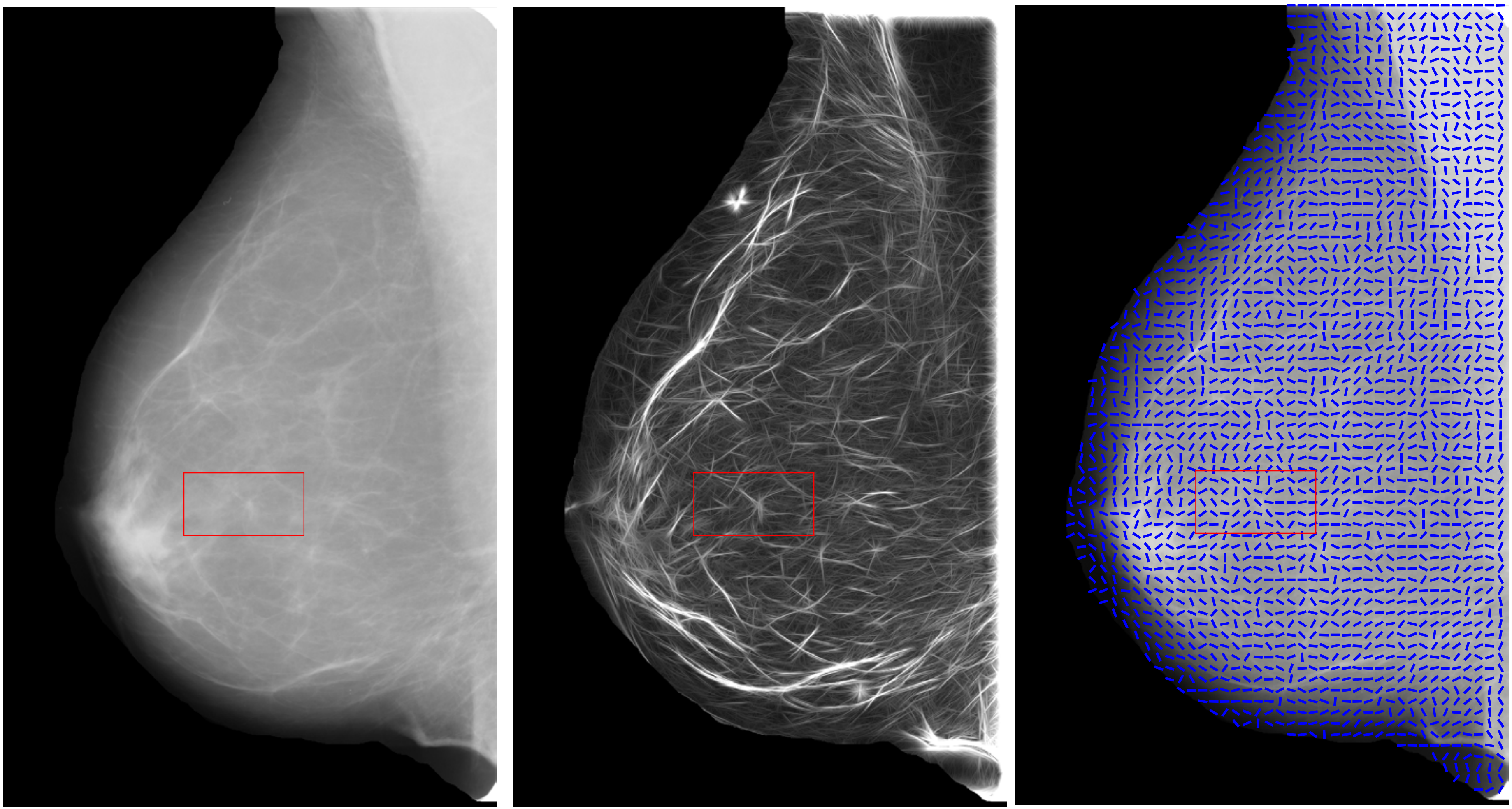

Original image *Gabor magnitude* *Gabor angle*

Divergence with Respect to the Expected Loci of Breast Tissue

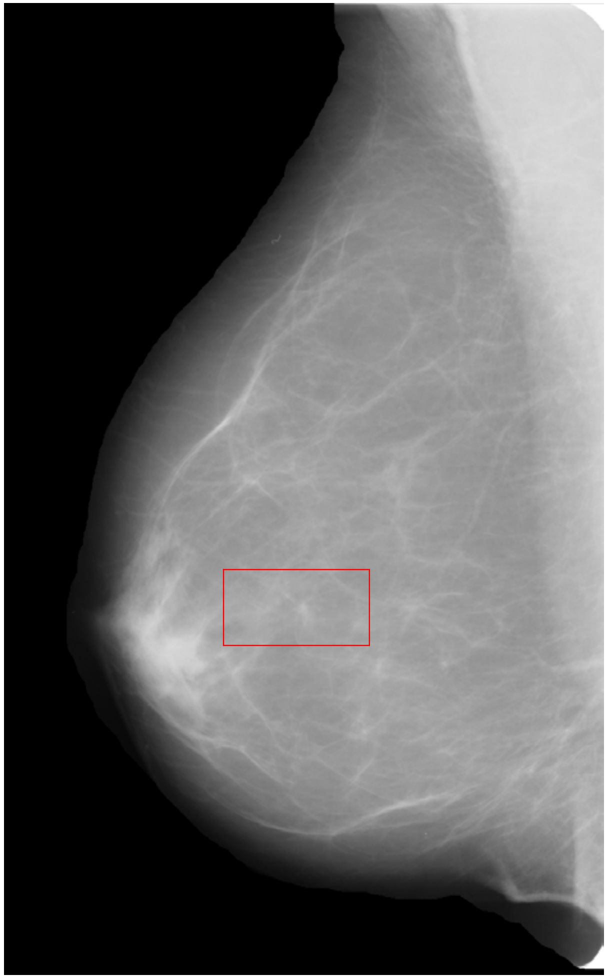

Original image

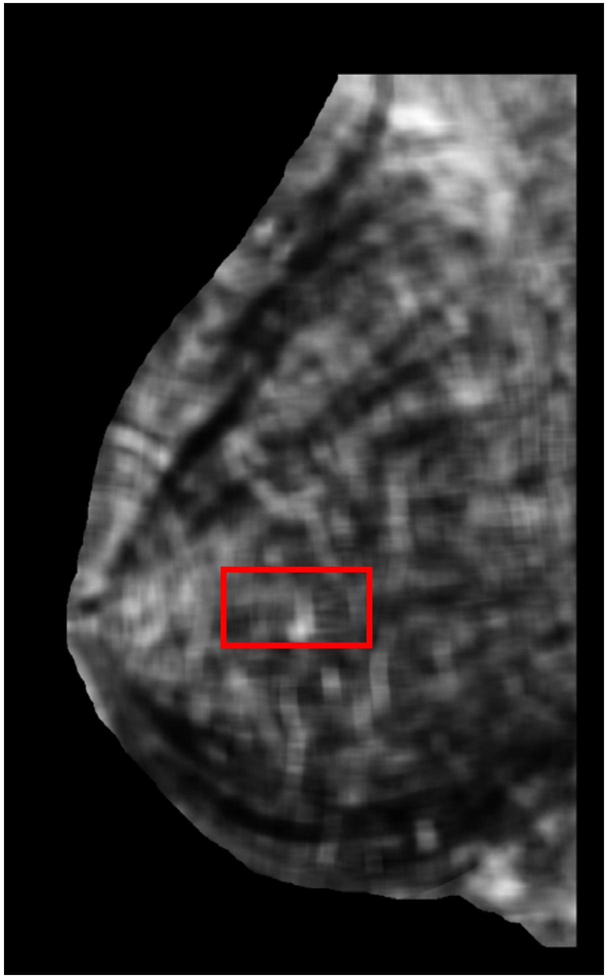

Divergence map

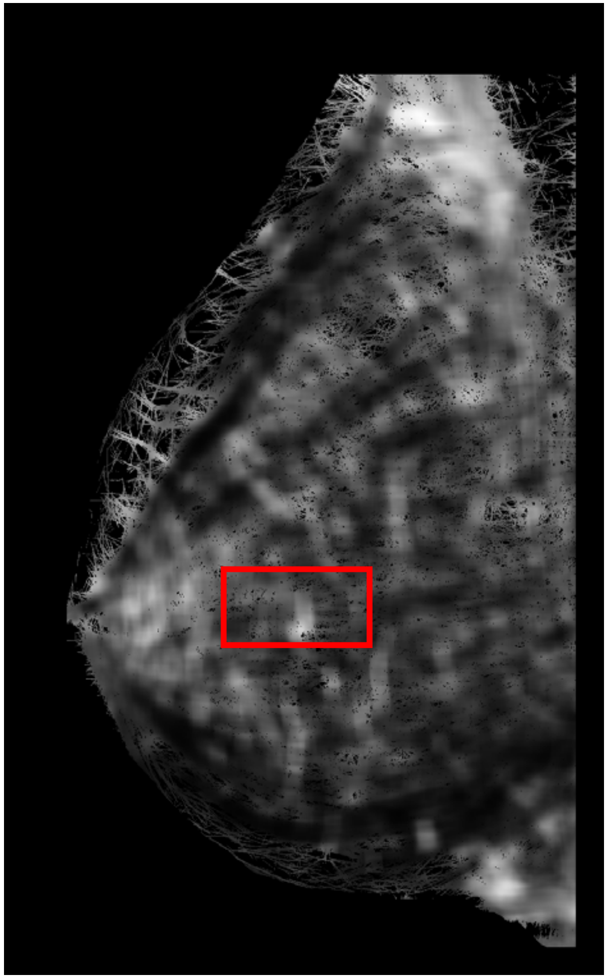

Thresholded map

Automatically Detected Regions of Interest

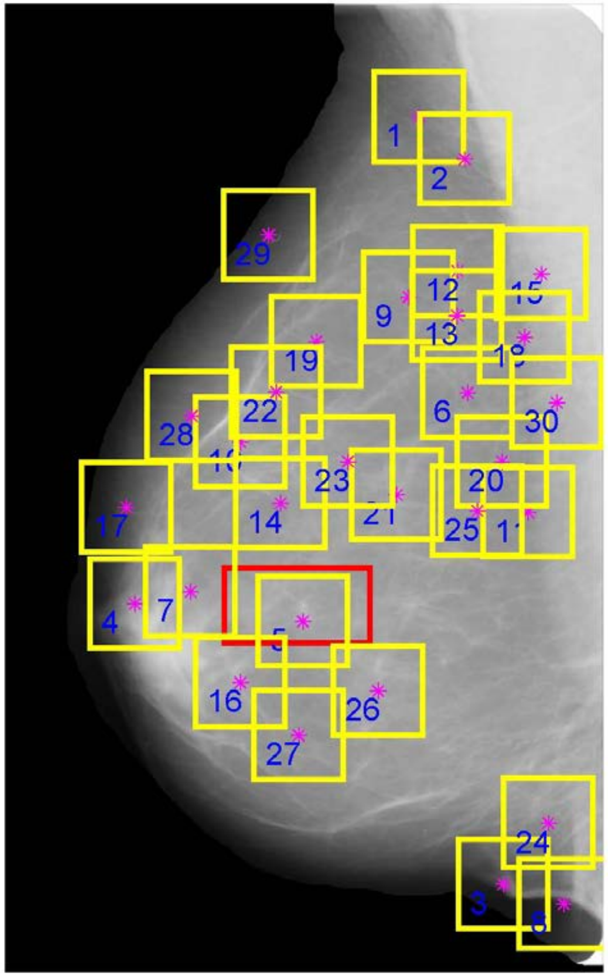

ROC:
AUC = 0.61

FROC:
Sensitivity = 80%
at 9.1 FP/patient

Performance of Selected Features

Initial number of ROIs selected	Feature selection using stepwise logistic regression				Using all of the 12 features proposed			
	ROC analysis (AUC)		FROC analysis (FP/patient at the sensitivities shown)		ROC analysis (AUC)		FROC analysis (FP/patient at the sensitivities shown)	
	Bayesian	ANN	80%	90%	Bayesian	ANN	80%	90%
30	0.74	**0.75**	**5.3**	6.6	0.69	0.71	5.9	7.7
25	0.73	0.73	6.0	7.5	0.68	0.68	5.6	7.1
20	0.70	0.70	6.7	8.0	0.67	0.69	5.8	7.0
15	0.71	0.73	5.8	7.3	0.67	0.70	5.7	6.5

FROC Performance of Features

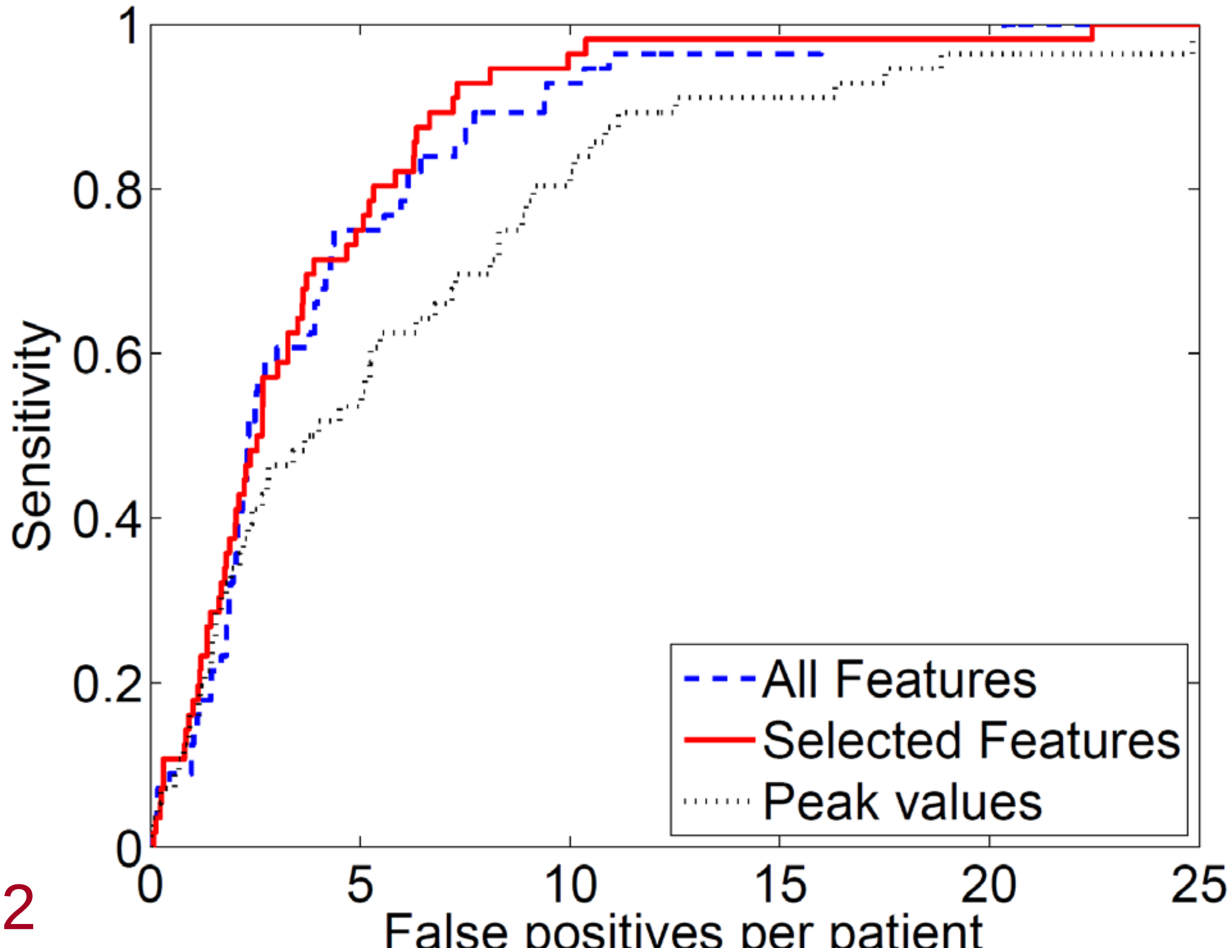

IJCARS 2012

Combination of 86 Features

- Spiculation features IDS, RWD, AWD, AWDES: 12
- Haralick's and Laws' texture features, fractal dimension: 25
- Angular spread, entropy: 15
- Haralick's measures with angle cooccurrence matrices: 28
- Statistical measures of angular dispersion and correlation: 6
- Feature selection with stepwise logistic regression
- Bayesian classifier with leave-one-patient-out validation: **80% sensitivity at 3.7 FP/patient** (IJCARS 2012)

UNIVERSITY OF CALGARY

Reduction of False Positives

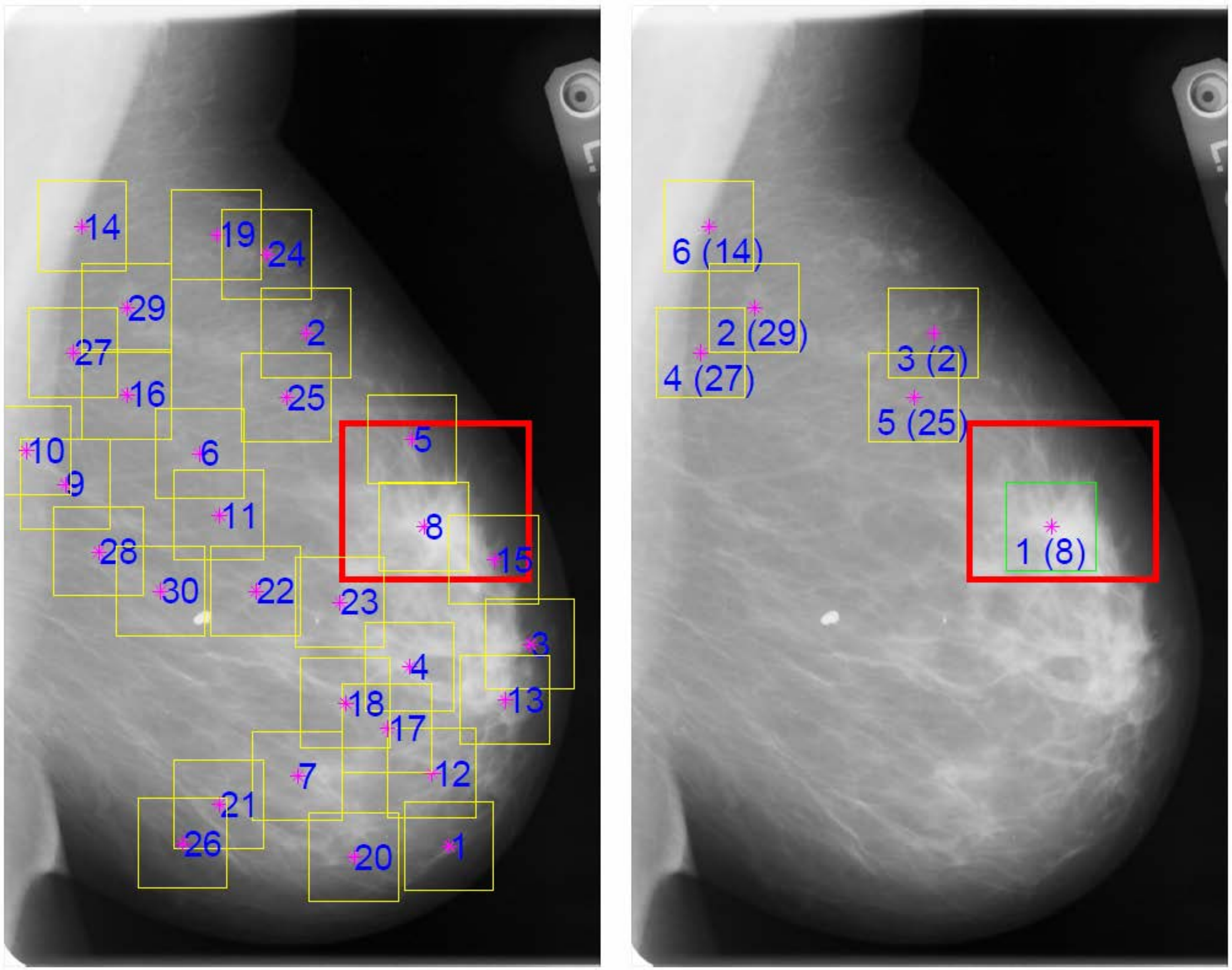

Reduction of False Positives

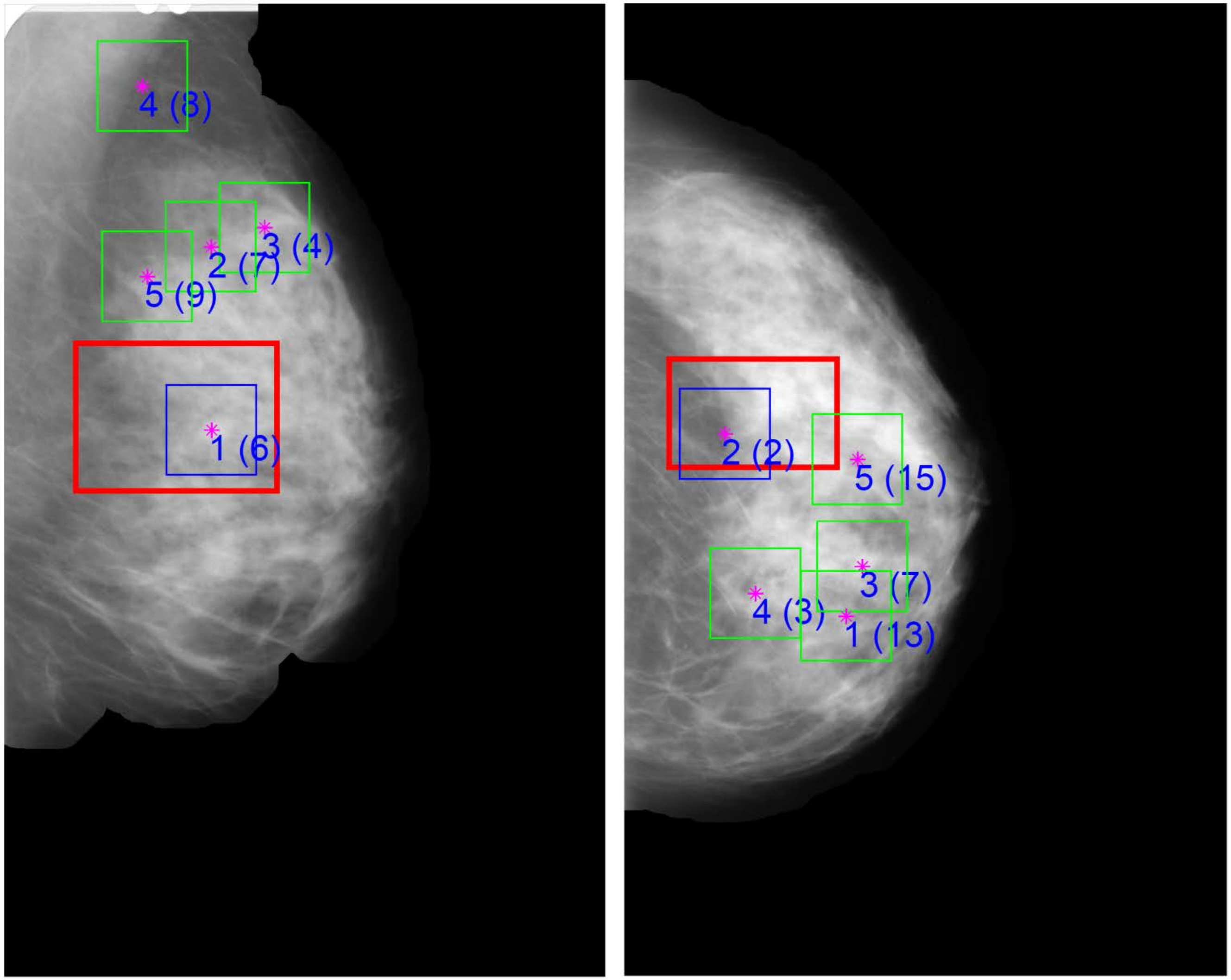

Conclusion

"Our methods can detect early signs of breast cancer 15 months ahead of the time of clinical diagnosis with a sensitivity of 80% with fewer than 4 false positives per patient"

- Future work:
  - Detection of sites of architectural distortion at higher sensitivity and lower false-positive rates
  - Application to direct digital mammograms and breast tomosythesis images

Thank You!

- Natural Sciences and Engineering Research Council (NSERC) of Canada
- Indian Institute of Technology Kharagpur
- Shastri Indo-Canadian Institute
- University of Calgary International Grants Committee
- Department of Information Technology, Government of India
- My collaborators and students:

  Dr. J.E.L. Desautels, Dr. S. Mukhopadhyay, N. Mudigonda, H. Alto, F.J. Ayres, S. Banik, S. Prajna, J. Chakraborty

http://people.ucalgary.ca/~ranga/